Entropy as a Property and Process in Understanding and Modeling Weather and Climate; Retrospection and Introspection

Donald R. Johnson
University of Wisconsin

Presentation at the 4th Hybrid Modeling Workshop

7 October 2008

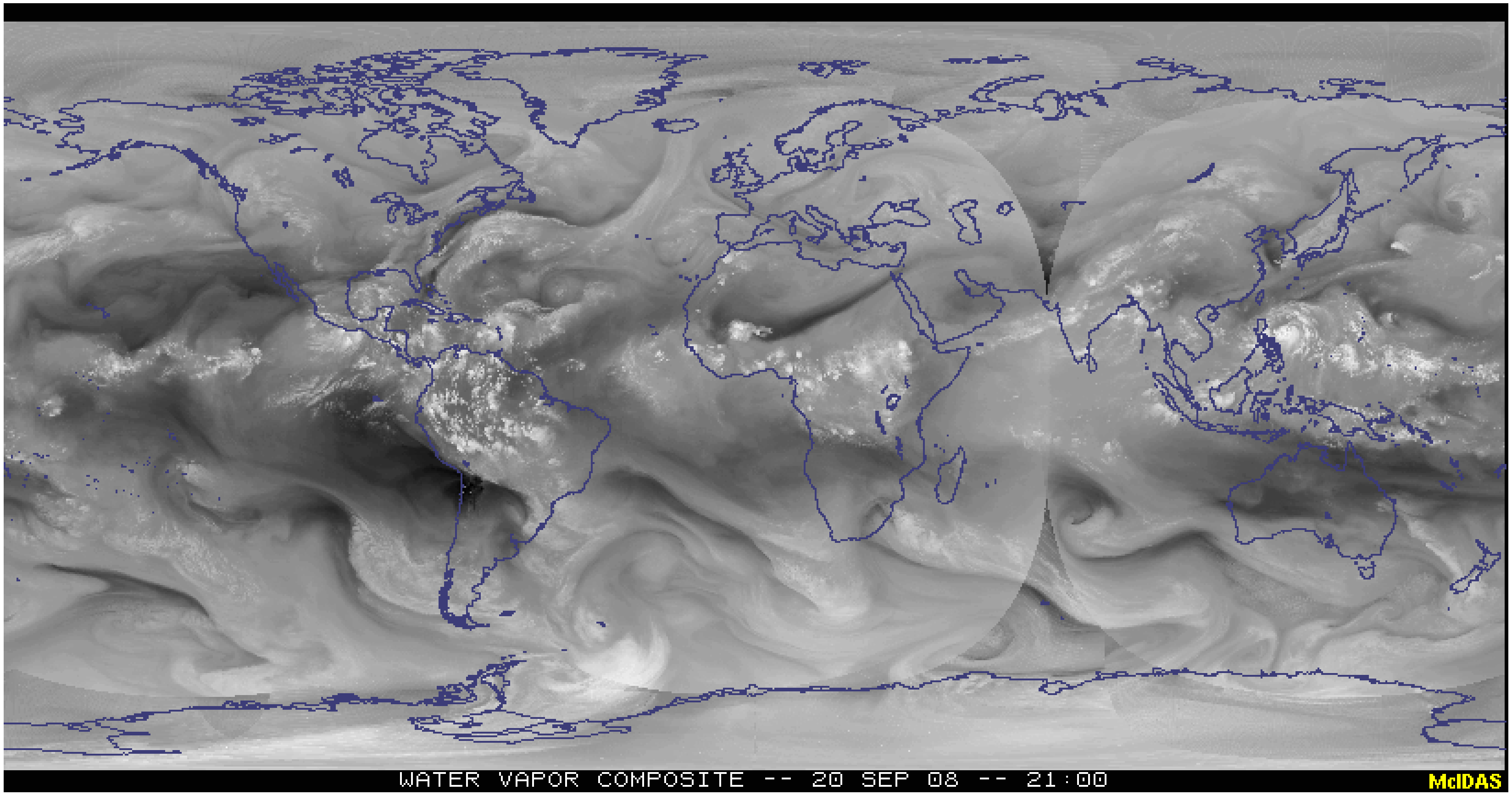
WATER VAPOR COMPOSITE -- 20 SEP 08 -- 21:00
McIDAS

Modeling and Analysis of the Earth's Hydrologic Cycle

Donald R. Johnson   Tom H. Zapotocny   Todd K. Schaack   Allen J. Lenzen

Space Science and Engineering Center, University of Wisconsin – Madison

Introduction

A key aim of this research is to further understanding of global water vapor and inert trace constituent transport in relation to climate change through analysis of simulations produced by the global University of Wisconsin (UW) hybrid isentropic-sigma coordinate models. Advancing the accuracy of the simulation of water substances, aerosols, chemical constituents, potential vorticity and stratospheric-tropospheric exchange are all critical to DOE's goal of accurate climate prediction on decadal to centennial time scales and assessing anthropogenic effects. Research has established that simulations of the transport of water vapor, and inert and chemical constituents are remarkably more accurate in hybrid isentropic coordinate models than in corresponding sigma coordinate models.

Primary Objectives:

- Advance the modeling of climate change by developing an isentropic hybrid model for global and regional climate simulations.
- Advance the understanding of physical processes involving water substances and the transport of trace constituents.
- Diagnostically examine the limits of global and regional climate predictability imposed by inherent limitations in the simulation of trace constituent transport, hydrologic processes and cloud life-cycles.

Key Findings:

- The results demonstrate the viability of the UW θ−η model for long term climate integration, numerical weather prediction and chemistry.
- The studies document that no insurmountable barriers exist for realistic simulations of the climate state with the hybrid vertical coordinate.
- Experiments reported here demonstrate a high degree of numerical accuracy for the UW θ−η model in simulating reversibility and potential vorticity transport over 10 day period that corresponds to the global residence time of water vapor.
- The UW hybrid θ−η model simulates seasonally varying and interannual climate scales realistically, including monsoonal circulations associated with El Nino/La Nina events.

Selected References

Schaack, T. K., T. H. Zapotocny, A. J. Lenzen and D. R. Johnson, 2004: Global climate simulation with the University of Wisconsin global hybrid isentropic coordinate model. Accepted for publication in *Journal of Climate.*

Johnson, D. R., A. J. Lenzen, T. H. Zapotocny and T. K. Schaack, 2002: Entropy, numerical uncertainties and modeling of atmospheric hydrologic processes: Part B. *J. Climate*, 15, 1777-1804.

Johnson, D. R., A. J. Lenzen, T. H. Zapotocny, and T. K. Schaack, 2000: Numerical uncertainties in the simulation of reversible isentropic processes and entropy conservation. *J. Climate*, 13, 3860-3884.

Johnson, D. R., 2000: Entropy, the Lorenz Energy Cycle and Climate. In "*General Circulation Model Development: Past, Present and Future*" (D. A. Randall, ed.), Academic Press, pp. 659-720.

Reames, F. M. and T. H. Zapotocny, 1999a: Inert trace constituent transport in sigma and hybrid isentropic-sigma models. Part I: Nine advection algorithms. *Mon. Wea. Rev.*, 127, 173-187.

Reames, F. M. and T. H. Zapotocny, 1999b: Inert trace constituent transport in sigma and hybrid isentropic-sigma models. Part II: Twelve semi-Lagrangian algorithms. *Mon. Wea. Rev.*, 127, 188-200.

Johnson, D. R., 1997: On the "General Coldness of Climate Models" and the Second Law: Implications for Modeling the Earth System. *J. Climate*, 10, 2826-2846.

Zapotocny, T. H., A. J. Lenzen, D. R. Johnson, F. M. Reames, and T. K. Schaack, 1997a: A comparison of inert trace constituent transport between the University of Wisconsin isentropic-sigma model and the NCAR community climate model. *Mon. Wea. Rev.*, 125, 120-142.

Zapotocny, T. H., D. R. Johnson, T. K. Schaack, A. J. Lenzen, and F. M. Reames, and P. A. Politowicz, 1997b: Simulations of Joint Distributions of Equivalent Potential Temperature and an Inert Trace Constituent in the UW θ−σ Model and CCM2. *Geophys. Res. Lett.*, 24, 865-868.

Zapotocny, T. H., A. J. Lenzen, D. R. Johnson, F. M. Reames, P. A. Politowicz, and T. K. Schaack, 1996: Joint distributions of potential vorticity and inert trace constituent in CCM2 and UW θ−σ model simulations. *Geophys. Res. Lett.*, 23, 2525-2528.

Zapotocny, T. H., D. R. Johnson, and F. M. Reames, 1994: Development and initial test of the University of Wisconsin global isentropic-sigma model. *Mon. Wea. Rev.*, 122, 2160-2178.

A. Design of Model Vertical Coordinate

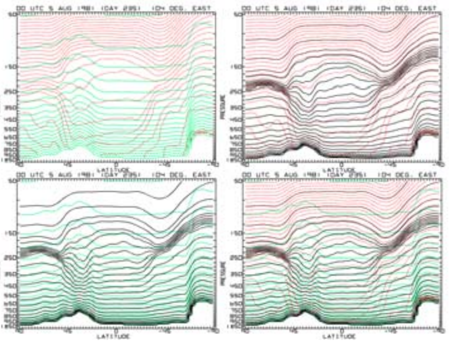

Fig. 1. Schematic of meridional cross sections along 104E for 05 August 1981. The red lines represent potential temperature; the black lines represent UW θ−η model surfaces; the green lines represent scaled sigma model surfaces.

B. Accuracy Analysis of Transport and Revers......

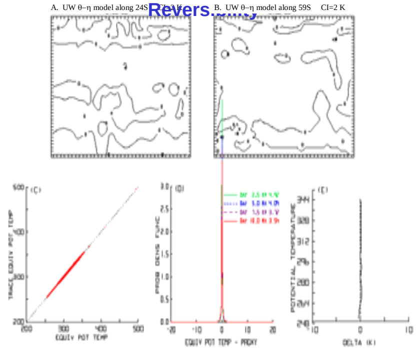

Fig. 2. The top two panels show zonal cross sections of the difference between θe and trace θe (CI=2 K) from the UW θ−η model at day 10. Panel C shows a bivariate distribution of θe and trace θe at day 10, panel D shows a relative frequency distribution of simulated differences between θe and trace θe at days 2.5, 5, 7.5 and 10, and panel E shows a vertical profile of the differences at day 10.

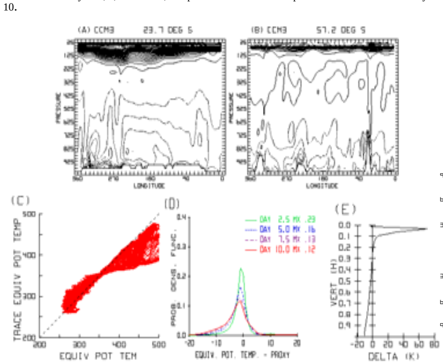

Fig. 3. Same as Fig. 2 except for CCM3 running at T42 horizontal resolution.

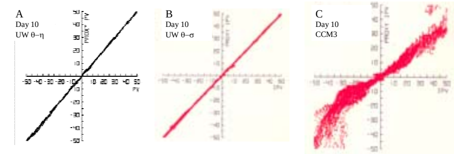

Fig. 4. Bivariate distributions of ozone and a proxy trace ozone. The "Day 10" distributions from the UW θ−η model, UW θ−σ model, and T42 CCM3 are shown in panels (A)-(C) respectively.

Table 1. Results from analysis of variance globally for the difference of equivalent potential temperature minus its trace (θe-t θe) and three components at day 10. Units of variance are the square of Kelvin temperature (K^2). Quantity in parenthesis is the RMS temperature difference (±K).

UW Hybrid Model

UW θ−σ	0.70(0.84)	0.23(0.48)	0.13(0.35)	1.05 (1.03)
UW θ−η	0.12 (0.35)	0.01 (.10)	0.03 (.16)	0.16 (0.40)

CCM2 and CCM3

	$S_G(\theta^*)$	$S_G(\bar{\theta}^*)$	$S_G(\bar{\bar{\theta}})$	$S_G(\theta)$
CCM3	37.45 (6.12)	195.77 (13.99)	0.02 (.15)	233.24 (15.27)
CCM3/2	27.88 (5.28)	0.09 (0.30)	0.03 (0.16)	28.00 (5.29)
CM2(all spectral)	10.83 (3.29)	2.12 (1.46)	15.03 (3.88)	27.98 (5.29)
CCM3(all semi-Lagrangian)	3.41 (1.85)	0.64 (0.79)	0.03 (0.16)	4.08 (2.02)

CCM3

CCM3 Standard	37.45 (6.12)	195.77 (13.99)	0.02 (.15)	233.24 (15.27)
CCM3 Modified	5.93 (2.44)	0.25 (.50)	0.01 (.09)	6.19 (2.49)

The first three columns respectively list the variances of 1) the differences about the area mean difference, 2) area mean differences about the grand mean difference and 3) the variance of the grand mean difference. The last column lists the total variance of the differences.

C. UW θ−η Climate Simulations

Table 2. A comparison of annually averaged fields from the 13-year UW θ−η model climate simulation to observed values. Observational estimates are from a summary by Hack et al. 1998.

Field	Observed	UW θ−η model
All sky OLR ($W\ m^{-2}$)	234.8	238.4
Clear sky OLR ($W\ m^{-2}$)	264.0	266.3
Total cloud forcing ($W\ m^{-2}$)	-19.0	-13.4
Longwave cloud forcing ($W\ m^{-2}$)	29.2	27.9
Shortwave cloud forcing ($W\ m^{-2}$)	-48.2	-41.3
Total Cloud fraction (%)	52.2 to 62.5	60.7
Precipitable water (mm)	24.7	22.8
Precipitation ($mm\ day^{-1}$)	2.7	3.1
Latent heat flux ($W\ m^{-2}$)	78.0	89.9
Sensible heat flux ($W\ m^{-2}$)	24.0	16.3

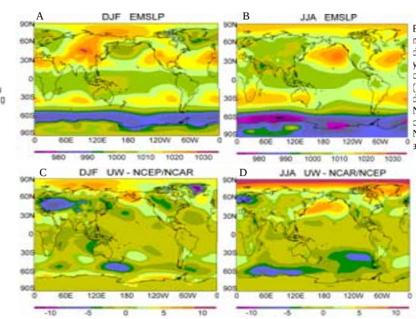

Fig. 5. The time averaged mean sea-level pressure distributions from the 13 year UW θ−η model climate simulation for DJF (A) and JJA (B) as well as differences from the NCEP/NCAR reanalysis climatology (UW-NCEP/NCAR) for DJF (C) and JJA (D).

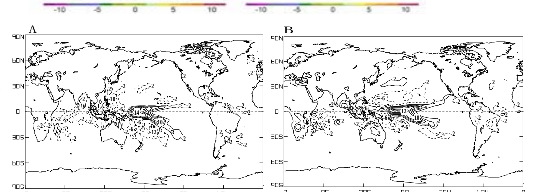

Fig. 6. Global distributions of the difference (DJF 1987-88 minus DJF 1988-89) between seasonally average precipitation for DJF 1987-88 and DJF 1988-89 (mm/day) from the (A) Xie and Arkin (1997) climatologic and (B) UW θ−η model climate simulation.

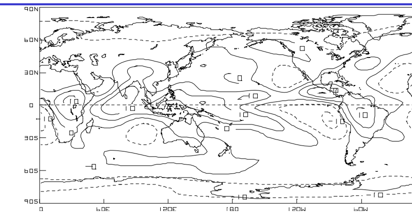

Fig. 7. The distribution of annual vertically averaged heating (10^{-1} K/Day) from the last 13 years of a 14 year climate run with UW θ−η model.

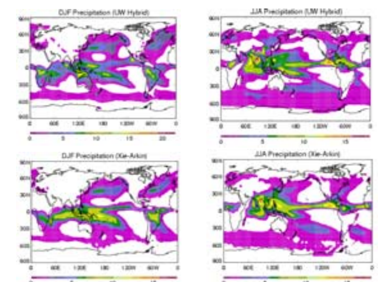

Fig. 8. The time averaged distributions of precipitation (mm/day) from the 13 year UW θ−η model climate simulation for DJF (A) and JJA (B) and from the Xie and Arkin precipitation climatology for 1979-99 for DJF (C) and JJA (D).

D. NCEP and NASA Collaborative Studies

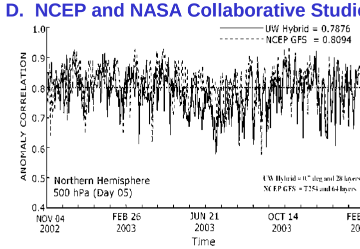

Fig. 9. Fifteen month record of Anomaly Correlation from the UW θ−η model and NCEP Global Forecast System.

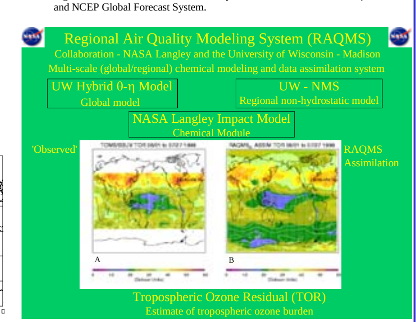

Fig 10. The UW hybrid model forms the global component of the RAQMS data assimilation system. Figure B shows tropospheric ozone burden (DU) for June-July 1999 from the RAQMS assimilation while Fig. A is the satellite observed estimate.

The presentation is dedicated to the memory of Professor Heinz Lettau, who within his lectures presented the derivation of the Navier Stokes equations based on the Maxwell-Boltzmann velocity distribution law from the kinetic theory of gases.

Professor Lettau not only authored the first book on atmospheric turbulence in 1939, but demonstrated understanding of the 2nd Law by estimating the global dissipation of kinetic energy though assessing the increase of entropy. Throughout his career he demonstrated his command of the underlying principles in enumerable applications ranging from micro to global scales of atmospheric circulation.

By

DAVID BRUNT, M.A., Sc.D., F.R.S.

Professor of Meteorology in the University of London, late Superintendent of the Army Meteorological Services, Air Ministry, London

CAMBRIDGE
AT THE UNIVERSITY PRESS
1941

CERTIFIED TO BE PERSONAL PROPERTY

OF Maj. Heinz LeHan 31G 14602

Vickers B. Watts

1st Lt AUS

Censored

PW Camp, Ruston, La.

By

Schematic of Atmospheric Energy Reservoirs and Renewal

Prepared by Professor Heinz Lettau, University of Wisconsin-Madison and shared with Donald Johnson in the mid 1960's. (See note dated without year)

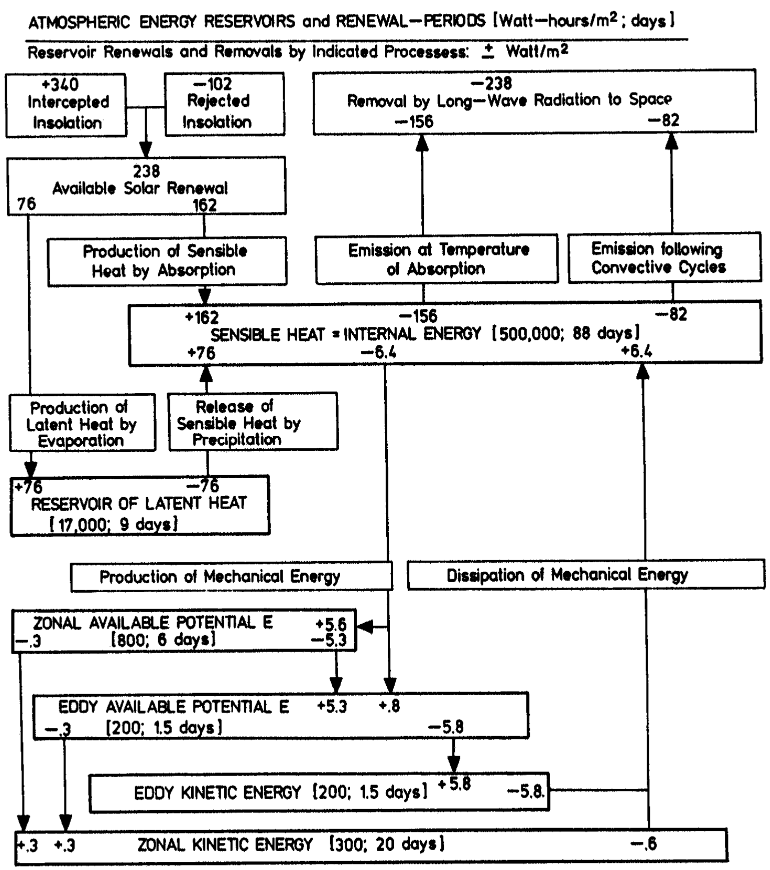

Schematic of Atmospheric Energy Reservoirs and Renewal (Continued)

Two references to Professor Lettau's interests in the balance of mass, momentum and energy for the global atmosphere circulation are:

Lettau, H. (1954a). A study of the mass, momentum and energy budget of the atmosphere. *Archiv. Meteor. Geophys. Bioklima.*, A, **7**, 133-157.

Lettau, H. (1954b). Notes on the transformation of mechanical energy from eddying motion. *J. Meteorol.*, **11**, 196-201.

Discussions in the 60's focused on the thermal forcing of the atmosphere's global circulation and its maintenance against kinetic energy dissipation. These discussions were crucial to the development of isentropic perspectives of global monsoonal circulations.

Note from Professor Lettau.

3/5

Don:
For your information!
As you can see, I
reduced the
Eddy Reservoirs only
for a Flip-Flop!

H. L.

global mean temperature error DJF0001

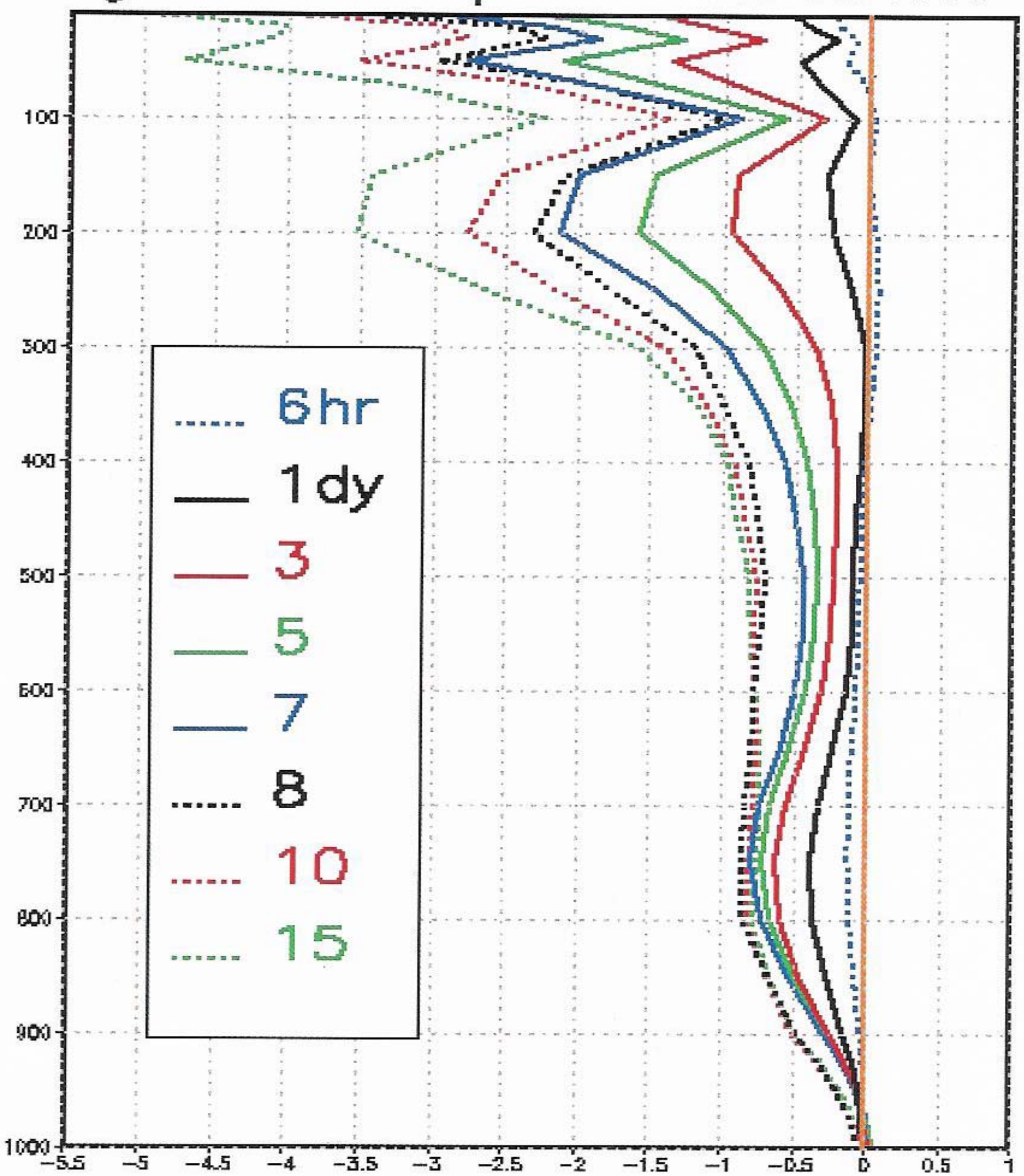

GrADS: COLA/IGES

2001-03-07-10:18

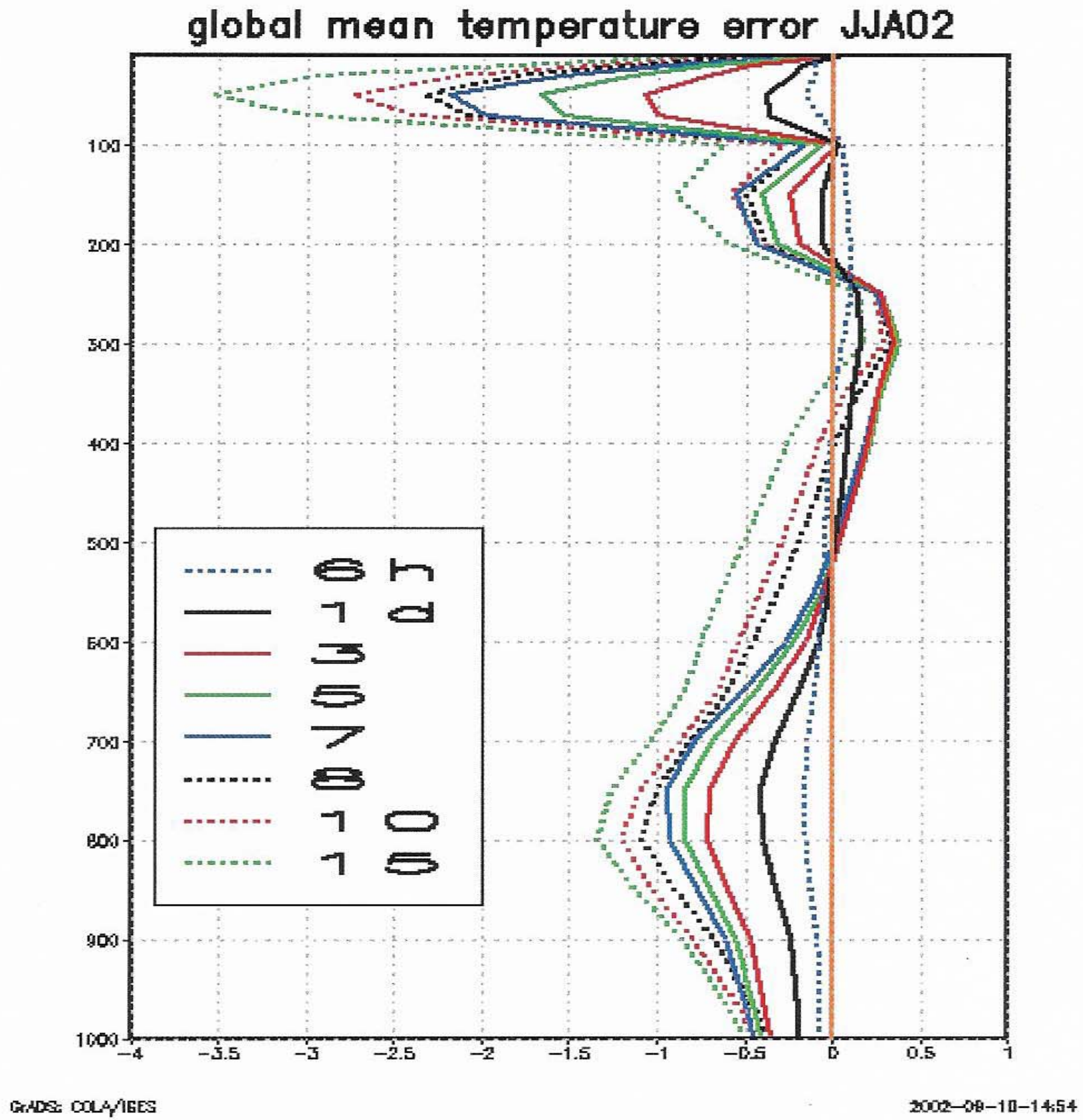

global mean temperature error JJA02
100
200
300
400
500
600
700
800
900
1000
-4
-3.5
-3
-2.5
-2
-1.5
-1
-0.5
0
0.5
1
6 h
1 d
3
5
7
8
10
15
GrADS: COLA/IGES
2002-09-10-14:54

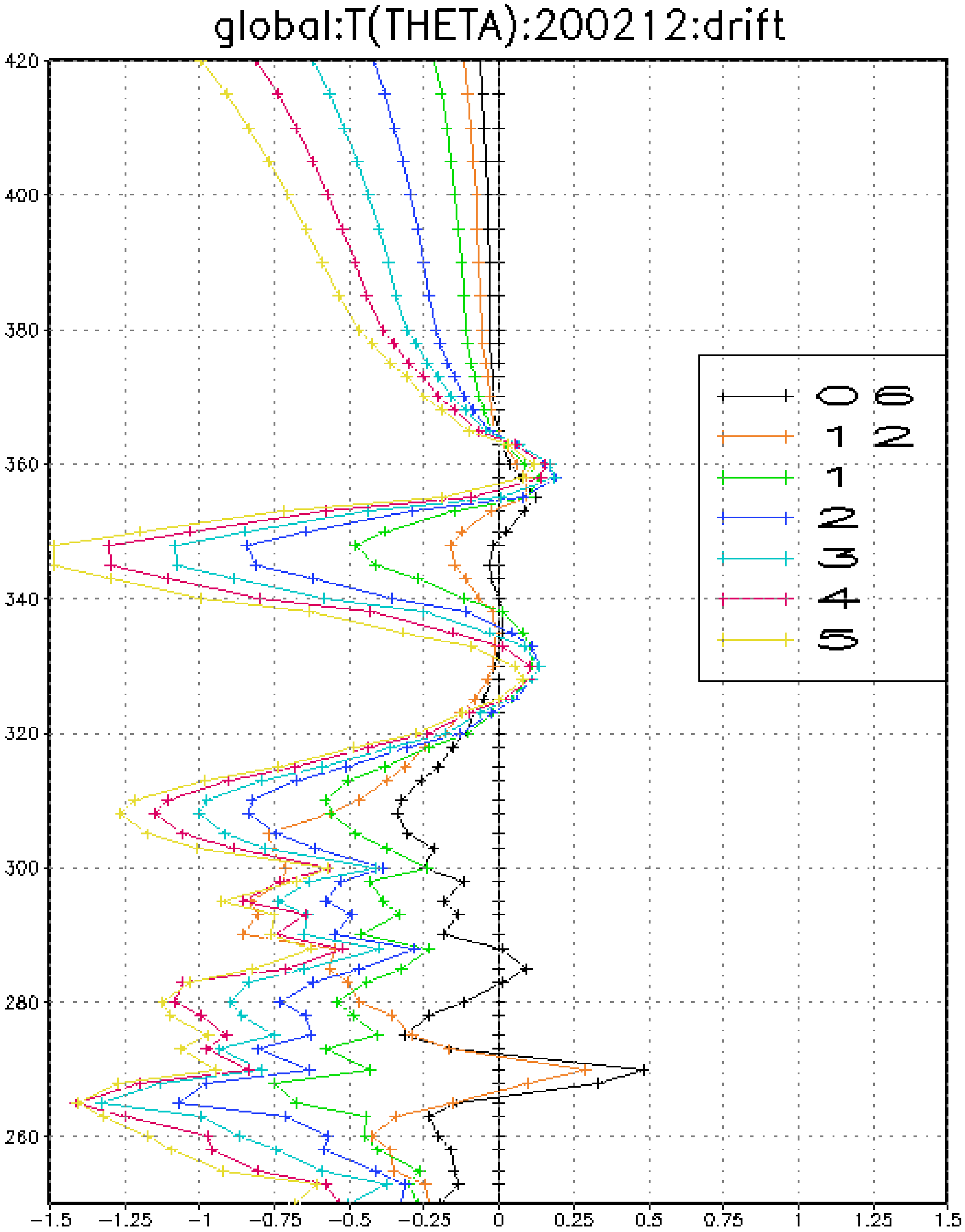

global:T(THETA):200212:drift
420
400
380
360
340
320
300
280
260
-1.5
-1.25
-1
-0.75
-0.5
-0.25
0
0.25
0.5
0.75
1
1.25
1.5
06
12
1
2
3
4
5

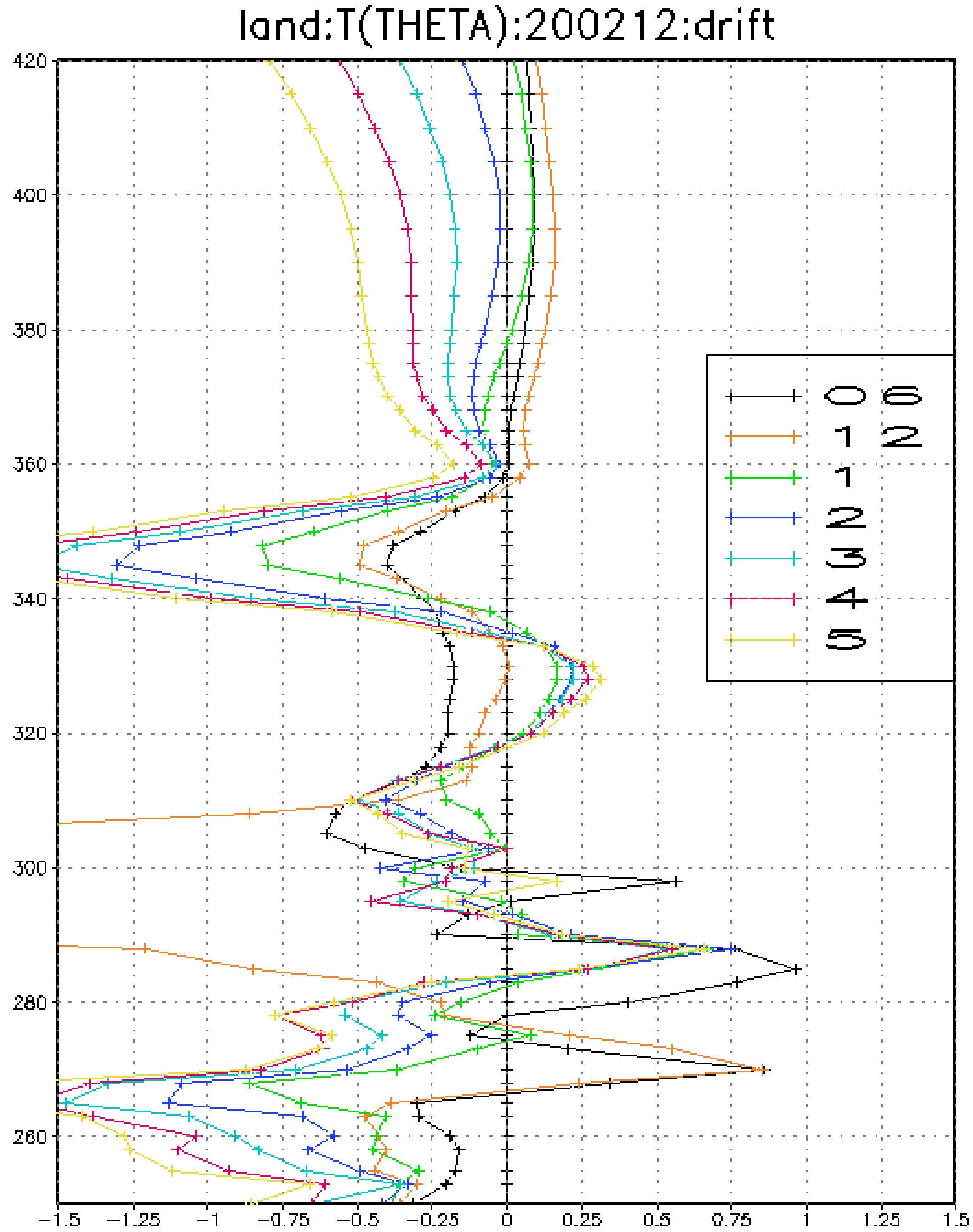
land:T(THETA):200212:drift
420
400
380
360
340
320
300
280
260
−1.5
−1.25
−1
−0.75
−0.5
−0.25
0
0.25
0.5
0.75
1
1.25
1.5
0 6
1 2
1
2
3
4
5

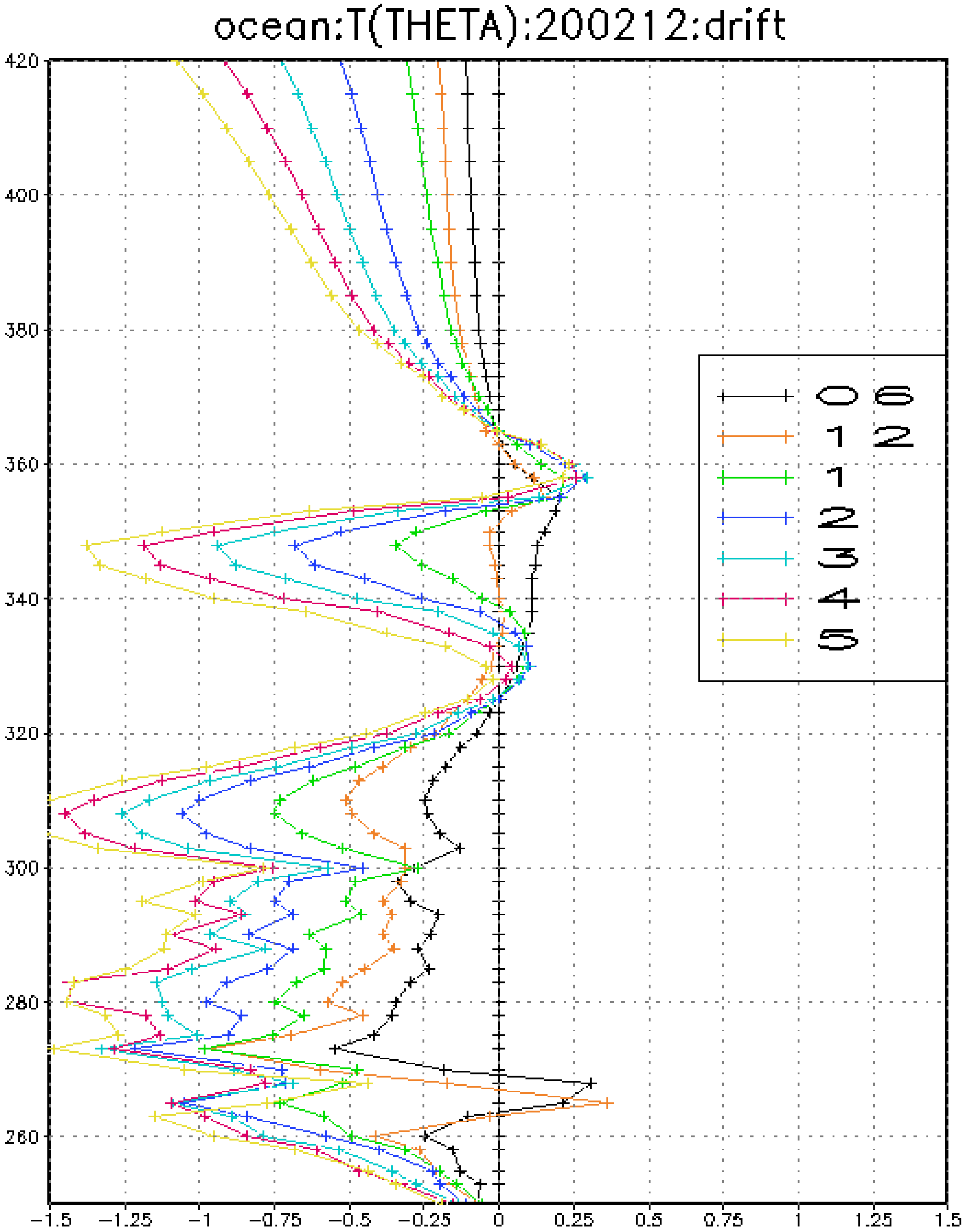

ocean:T(THETA):200212:drift
420
400
380
360
340
320
300
280
260
−1.5
−1.25
−1
−0.75
−0.5
−0.25
0
0.25
0.5
0.75
1
1.25
1.5
0 6
1 2
1
2
3
4
5

Caratheodory'statement of the Second Law (Sommerfeld 1950)

"In the neighborhood of every state which can be reached reversible , there exists states which cannot be reached along a reversible adiabatic path, or in other words, which can only be reached irreversible or which cannot be reached at all."

Is Caratheodory's statement of the Second Law relevant to modeling of the climate state? If so, are there robust means to assess the accuracies of model in appropriately simulating reversibility, or alternatively to avoid adjacent states that should not be reached by irreversible processes?

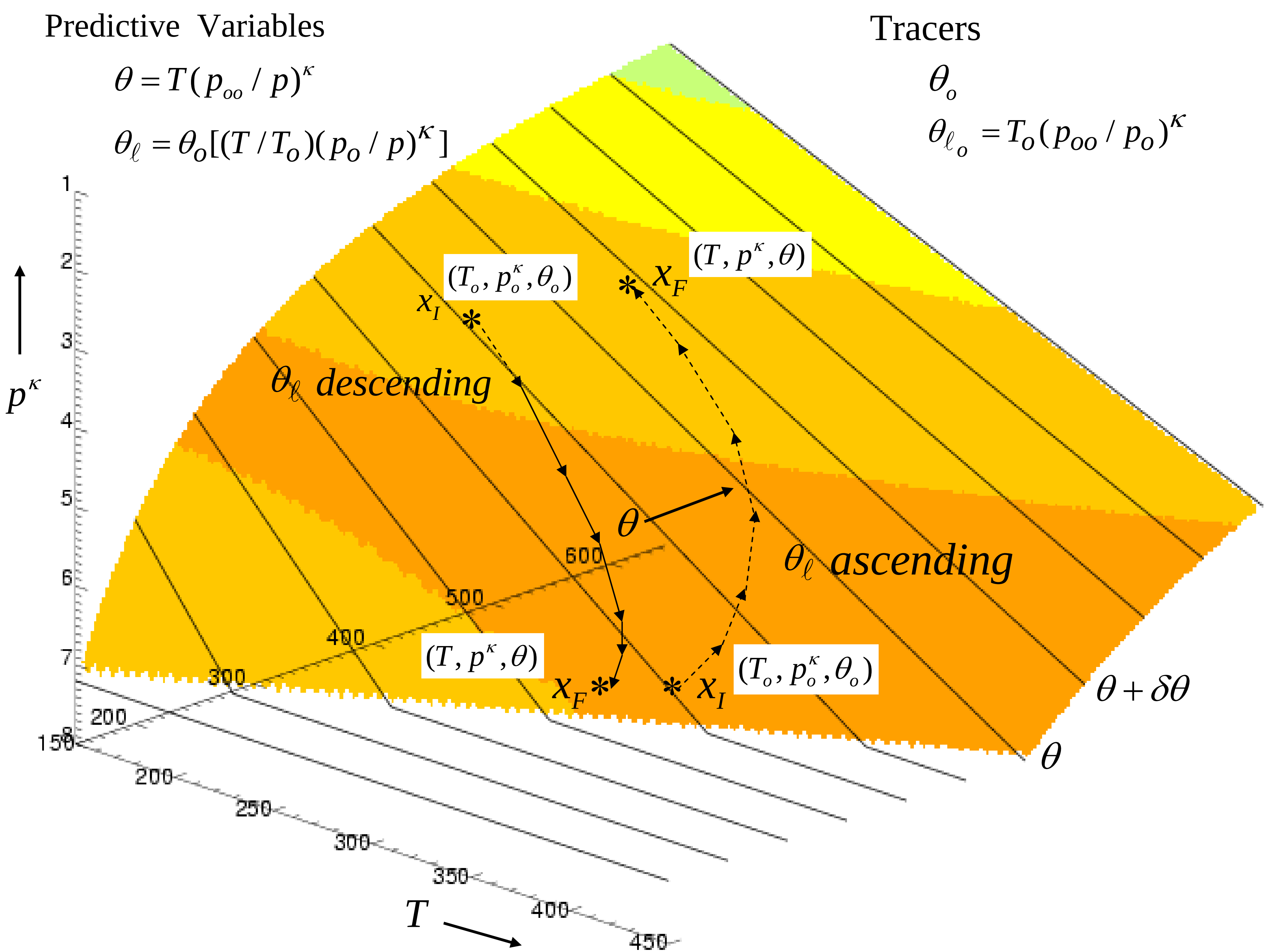

Predictive Variables
$\theta = T(p_{oo}/p)^{\kappa}$
$\theta_\ell = \theta_o[(T/T_o)(p_o/p)^{\kappa}]$
Tracers
θ_o
$\theta_{\ell_o} = T_o(p_{oo}/p_o)^{\kappa}$
p^{κ}
T
$(T_o, p_o^{\kappa}, \theta_o)$
x_I
(T, p^{κ}, θ)
x_F
θ_ℓ descending
θ_ℓ ascending
θ
$\theta + \delta\theta$

The Extended Proportion Defining *Carathéodory's Admissible Surfaces* *

$$\theta_\ell : \theta_o = (c_1 T_\ell^{1-\kappa}\alpha_\ell^{\kappa}) : (c_1 T_o^{1-\kappa}\alpha_o^{\kappa}) = (c_2 T_\ell / p_\ell^{\kappa}) : (c_2 T_o / p_o^{\kappa})] = (c_3 \alpha_\ell p_\ell^{1-\kappa}) : (c_3 \alpha_o p_o^{1-\kappa}) = (\theta / \theta_{\ell_o})$$

Carathéodory's Two Dimensional Surface as a function of (α, T, θ)

$$\sigma_{o1} = \sigma_1 = \frac{c_1(T^{1-\kappa}\alpha^{\kappa})}{\theta_\ell} = \frac{c_1\lambda_1}{\theta_\ell} = \frac{\theta(c_1, T, \alpha)}{\theta_\ell} = \frac{\theta_{\ell_o}(c_1, T_o, \alpha_0)}{\theta_o}$$

$$c_1 = (p_{oo} / R)^{\kappa}$$

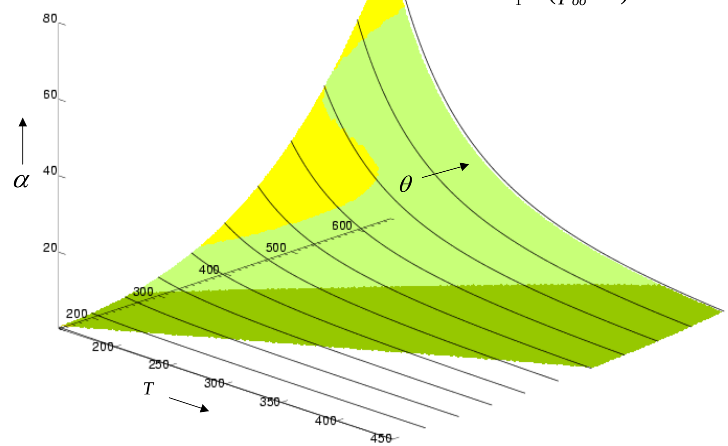

Carathéodory's Two Dimensional Surface as a function of (T, p, θ)

$$\sigma_{o2} = \sigma_2 = \frac{c_2(T / p^{\kappa})}{\theta_\ell} = \frac{c_2\lambda_2}{\theta_\ell} = \frac{\theta(c_2, T, p^{\kappa})}{\theta_\ell} = \frac{\theta_{\ell_o}(c_2, T_o, p_o^{\kappa})}{\theta_o}$$

$$c_2 = (p_{oo}^{\kappa})$$

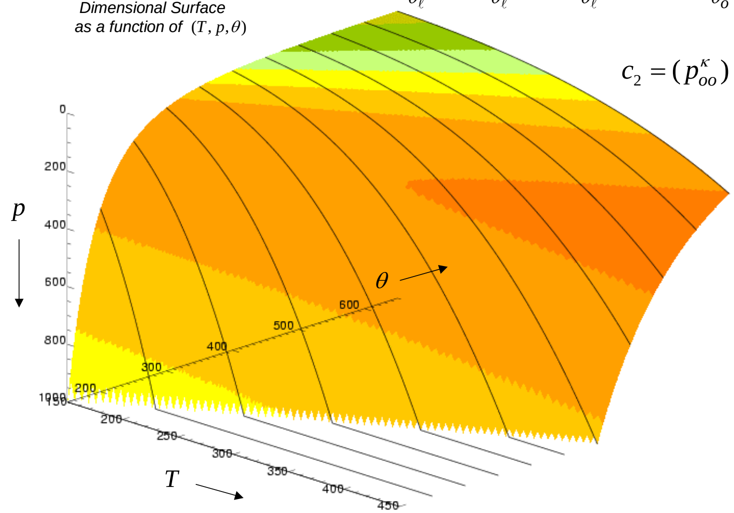

Carathéodory's Two Dimensional Surface as a function of (α, p, θ_ℓ)

$$\sigma_{o3} = \sigma_3 = \frac{c_3(\alpha p^{1-\kappa})}{\theta_\ell} = \frac{c_3\lambda_3}{\theta_\ell} = \frac{\theta(c_3, \alpha, p^{1-\kappa})}{\theta_\ell} = \frac{\theta_{\ell_o}(c_2, \alpha_o, p_o^{1-\kappa})}{\theta_o}$$

$$c_3 = (p_{oo}^{\kappa} / R)$$

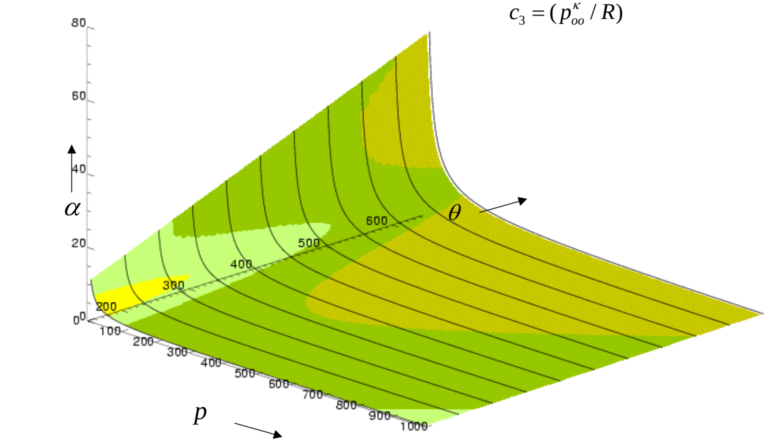

The Two Dimensional surface For the Ideal Gas Law

$$R = (p\alpha / T)$$

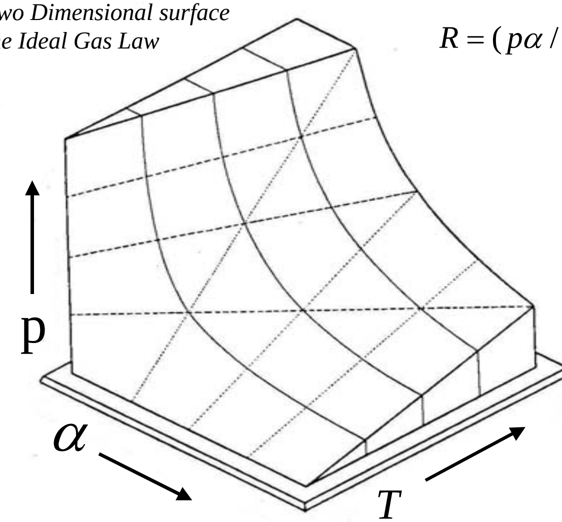

* Extracted from manuscript in preparation, Johnson (2007)

Now consider the global mean energy balance for the true atmosphere under the constraint of energy conservation as expressed by

$$\hat{\tilde{\dot{e}}} = [\hat{\tilde{Q}} - \hat{\tilde{d}}(k)], \qquad (11)$$

where $\hat{\tilde{\dot{e}}}(t)$ is the sum of the time dependent global mean specific Lagrangian time rate of change of specific internal $(u = c_v T)$, geopotential (ϕ) and kinetic (k) energies while $\hat{\tilde{d}}(k)$ is the time dependent global mean kinetic energy dissipation.

$$Q = \{\{\varepsilon^2 - [\nabla \cdot \underset{\sim}{H}_{lw} + \nabla \cdot \underset{\sim}{H}_{sw} + \nabla \cdot \underset{\sim}{H}_{sh} + \rho \frac{d}{dt}(Lq)]\} / \rho\}$$

$$\dot{s} = \{(\varepsilon^2 + T\mu^2) - [\nabla \bullet \underset{\sim}{H}_{lw} + \nabla \bullet \underset{\sim}{H}_{sw} + \rho \frac{d}{dt}(Lq)] + T\nabla \bullet [k(\ell nT)]\} / T\rho$$

$$\hat{\hat{\tilde{\dot{s}}}} = \hat{\hat{\tilde{d}}}(k) / \bar{\tilde{T}} > 0$$

$$\hat{\hat{\dot{s}}} = [\hat{\hat{d}}(k) / \bar{T}] > 0$$

$$\Delta\bar{T} = \lambda(\bar{T}) = [E(\bar{T}) - \bar{\tilde{T}}]$$

$$\bar{T}^{-1} = \bar{\tilde{T}}^{-1}(1 - (\Delta\bar{T} / \bar{\tilde{T}})$$

$$\hat{\hat{\dot{s}}} = [\hat{\hat{d}}(k) / \bar{\tilde{T}}](1 - (\Delta\bar{T} / \bar{\tilde{T}})] > 0$$

$$\left\langle \dot{\hat{\tilde{e}}} \right\rangle = \left\langle \overset{\square}{\tilde{T}}\ \dot{\tilde{s}} \right\rangle - \left\langle \hat{\tilde{d}}(k) \right\rangle = \left\langle \overset{\square}{\tilde{T}}\ \dot{\tilde{s}} \right\rangle - \hat{\hat{\tilde{d}}}(k) \tag{15a}$$

$$= \left\langle \bar{\tilde{T}}\ \dot{\hat{\tilde{s}}}) \right\rangle - \left\langle \hat{\tilde{d}}(k) \right\rangle = \bar{\bar{\tilde{T}}}\ \hat{\dot{\hat{\tilde{s}}}} + \left\langle \bar{\tilde{T}}^{+}\ \dot{\hat{\tilde{s}}}^{+}) \right\rangle - \hat{\hat{\tilde{d}}}(k) \tag{15b}$$

$$= [\left\langle \dot{\hat{\tilde{s}}}\ \hat{\tilde{T}} + \overset{\square}{\tilde{T}}^{***}\ \dot{\tilde{s}}^{***} \right\rangle - \left\langle \hat{\tilde{d}}(k) \right\rangle] = \hat{\dot{\hat{\tilde{s}}}}\hat{\hat{\tilde{T}}} + \left\langle \dot{\hat{\tilde{s}}}^{+}\ \hat{\tilde{T}}^{+} \right\rangle + \left\langle \overset{\square}{\tilde{T}}^{***}\ \dot{\tilde{s}}^{***} \right\rangle - \hat{\hat{\tilde{d}}}(k) \tag{15c}$$

$$\left\langle \dot{\hat{e}} \right\rangle = \left\langle \overset{\square}{T}\ \dot{s} \right\rangle - \left\langle \hat{\tilde{d}}(k) \right\rangle = \left\langle \overset{\square}{T}\ \dot{s} \right\rangle - \hat{\hat{\tilde{d}}}(k) \tag{16a}$$

$$= \left\langle \bar{T}\ \dot{\hat{s}} \right\rangle - \left\langle \hat{d}(k) \right\rangle = \bar{\bar{T}}\ \hat{\dot{\hat{s}}} + \left\langle \bar{T}^{+}\ \dot{\hat{s}}^{+}) \right\rangle - \hat{\hat{d}}(k) \tag{16b}$$

$$= \left\langle \hat{T}\ \dot{\hat{s}} + \overset{\square}{T}^{***}\ \dot{s}^{***} \right\rangle - \left\langle \hat{d}(k) \right\rangle = [\hat{\dot{\hat{s}}}\hat{\hat{T}} + \left\langle \dot{\hat{s}}^{+}\ \hat{T}^{+} \right\rangle + \left\langle \overset{\square}{T}^{***}\ \dot{s}^{***} \right\rangle] - \hat{\hat{d}}(k) \tag{16c}$$

$$\left\langle \hat{\tilde{d}}(k) \right\rangle = \left\langle \hat{\tilde{Q}} \right\rangle = \left\langle \tilde{T}\ \dot{\tilde{s}} \right\rangle = \bar{\bar{\tilde{T}}}\ \hat{\hat{\dot{\tilde{s}}}} = \hat{\hat{\dot{\tilde{s}}}}\hat{\tilde{T}} + \left\langle \tilde{T}^{***}\ \dot{\tilde{s}}^{***} \right\rangle, \tag{18}$$

$$\left\langle \hat{d}(k) \right\rangle = \left\langle \hat{Q} \right\rangle = \left\langle T\ \dot{s} \right\rangle = \bar{\bar{T}}\ \hat{\hat{\dot{s}}} = \hat{\hat{\dot{s}}}\hat{T} + \left\langle T^{***}\ \dot{s}^{***} \right\rangle. \tag{19}$$

$$\bar{\tilde{T}} = \hat{\hat{\tilde{T}}} + \left\langle \tilde{T}^{***}\ \dot{\tilde{s}}^{***} \right\rangle / \hat{\hat{\dot{\tilde{s}}}}, \tag{31a}$$

$$\bar{T} = \hat{\hat{T}} + \left\langle T^{***}\ \dot{s}^{***} \right\rangle / \hat{\hat{\dot{s}}}, \tag{31b}$$

Now a rearrangement of (32a) in the form of

$$\bar{\tilde{T}}^{-1} = [\langle \tilde{T}^{***}\tilde{\dot{s}}^{***}\rangle / (\bar{\tilde{T}} - \hat{\hat{\tilde{T}}})]/[\hat{\hat{\tilde{d}}}(k)]$$

followed by its substitution into (32b), an alternate relation corresponding with (32c) emerges as

$$\hat{\hat{\dot{s}}} = [\langle T^{***}\dot{s}^{***}\rangle / (\bar{T} - \hat{\hat{T}})] = \hat{\hat{d}}(k)\left\{\frac{[\langle \tilde{T}^{***}\tilde{\dot{s}}^{***}\rangle / (\bar{\tilde{T}} - \hat{\hat{\tilde{T}}})]}{\hat{\hat{\tilde{d}}}(k)}\right\}[1 - (\Delta\bar{T}/\bar{T})] \qquad (34)$$

Now under the condition of equality of the kinetic energy dissipation in the true and model states, (34) simplifies to

$$\hat{\hat{\dot{s}}} = [\langle T^{***}\dot{s}^{***}\rangle / (\bar{T} - \hat{\hat{T}})] = [\langle \tilde{T}^{***}\tilde{\dot{s}}^{***}\rangle / (\bar{\tilde{T}} - \hat{\hat{\tilde{T}}})]\,[1 - (\Delta\bar{T}/\bar{T})]$$

Now by addition and subtraction of the equilibrium temperature $T_{e_{A\theta}}$ within the deviation temperature $(T - \hat{T}^{A_\eta})$, the three dimensional deviation temperature defined by (37) is expressed by

$$T^{***} = [(T - T_{e_{A\theta}})^{***} + (T_{e_{A\theta}} - \hat{T}^{A_\eta})^{***}] + (\hat{T}^{A_\eta} - \hat{T}^{G})^{*} \qquad (39)$$

Within Lorenz's concept of available potential $T_{e_{A\theta}}$ is the equilibrium temperature defined by a virtual isentropic distribution of mass to a horizontally invariant reference state with uniformity of temperature and hydrostatic pressure relative to geopotential surfaces. In this study with its focus on internal energy and entropy, recognize that uniformity of temperature and entropy requires uniformity of pressure. Then the introduction of the hydrostatic equilibrium demands uniformity of pressure relative to geopotential surfaces. Interestingly, Chandrashkar's definition of local thermodynamic equilibrium of uniformity of internal energy and entropy only requires uniformity of pressure. However, when his definition of local thermodynamic equilibrium is combined with the hydrostatic constraint, the uniformity of geopotential energy as a requirement for local thermodynamic equilibrium enters. Thus the concept of Lorenz's reference state, which defines a minimum state for the sum of the internal and geopotential energies under the equilibrium of a hydrostatic constraint attained by a virtual isentropic redistribution of mass is actually a special case of local equilibrium of internal energy and entropy as defined by Chandrashkar. Concerning the relevance of the definition of local equilibrium states whether by Chandrashkar or Lorenz, it is extremely important to recognize that both are artifacts of the actual processes involved, however both serve to provide understanding of the relevance of just how the combination of internal energy as a state variable and entropy sources/sinks as internal processes maintain atmospheric circulation.

Now consider the efficiency factor (Dutton and Johnson 1967) determined by a virtual isentropic displacement of mass to a horizontally invariant reference state defined by

$$\varepsilon^{***} = [1 - (T_{e_{A_\theta}} / T)] = [1 - (p_{e_{A_\theta}} / p)^{\kappa}]. \tag{40}$$

Then recognize that ε^{***} is positive and negative when the temperature $T(\alpha, \beta, \eta, t)$ is respectively greater or less than the reference state temperature $T_{e_{A_\theta}}[\alpha, \beta, \theta(\alpha, \beta, \eta), t]$. Also consider that that the magnitude of the efficiency whether positive or negative is greater the greater the magnitude of the temperature deviations, that is the greater the magnitude of the efficiencies within the climate state, the greater is the thermal disequilibrium and the greater will be the impact of differential heating..

A multiplication of (40) by temperature and substitution into (39) yields

$$T^{***} = \{[(\varepsilon T)^{***} + (T_{e_{A_\eta}} - \hat{T}^{A_\eta})^{***}] + (\hat{T}^{A_\eta} - \hat{T}^{G})^{*}\} \tag{41}$$

Within this definition of efficiency as defined through the entropy principle, the paired variables $(T_{e_{A_\eta}}, p_{e_{A_\eta}})$ respectively represent the temperature and pressure of the time dependent areally invariant equilibrium state of available potential energy theory as determined by the internal energy and entropy distributions within the climate state.

Also by combining the second and third terms, and simple considering their sum as the deviation of the Lorenz reference state from the globally averaged internal energy in the form of $\overline{\widehat{\dot{s}^{A_\theta *}}}(T_{e_{A_\theta}} - \hat{T}^G)^*$ and $\overline{\widehat{\dot{s}^{A_\theta *}}}(\tilde{T}_{e_{A_\theta}} - \hat{\tilde{T}}^G)^*$, (47) reduces to

$$
\begin{aligned}
&\{\left\langle [\overline{\dot{s}^{***}}(\varepsilon_{A_\theta} T)^{***} + \overline{\widehat{\dot{s}^{A_\theta *}}}(T_{e_{A_\theta}} - \hat{T}^G)^*] \right\rangle\} / (\overline{T} - \hat{\hat{T}})\} \\
&= \{\left\langle [+\overline{\widetilde{\dot{s}^{***}}}(\tilde{\varepsilon}_{A_\theta} \tilde{T})^{***} + \overline{\widehat{\dot{s}^{A_\theta *}}}(\tilde{T}_{e_{A_\theta}} - \hat{\tilde{T}}^G)^* \right\rangle \} / (\overline{\tilde{T}} - \hat{\hat{\tilde{T}}})\}[1 - (\Delta \overline{T} / \overline{\tilde{T}})
\end{aligned}
\tag{48}
$$

Now under the condition that the cold bias $\Delta \overline{T}$ as defined is invariant in space and time under the condition of statistical equilibration, the difference $(\overline{T} - \hat{\hat{T}})$ within the model atmosphere is equal to the true state difference $(\overline{\tilde{T}} - \hat{\hat{\tilde{T}}})$, thus (48) simplifies to

$$
\begin{aligned}
&\{\left\langle [\overline{\dot{s}^{***}}(\varepsilon_{A_\theta} T)^{***} \right\rangle + \left\langle \overline{\widehat{\dot{s}^{A_\theta *}}}(\hat{T}_{e_{A_\theta}} - \hat{T}^G)^*] \right\rangle\} \\
&= \{\left\langle \overline{\widetilde{\dot{s}^{***}}}(\tilde{\varepsilon}_{A_\theta} \tilde{T})^{***} \right\rangle + \left\langle \overline{\widehat{\dot{s}^{A_\theta *}}}(\hat{\tilde{T}}_{e_{A_\theta}} - \hat{\tilde{T}}^G)^* \right\rangle \}[1 - (\Delta \overline{T} / \overline{\tilde{T}})
\end{aligned}
\tag{49}
$$

Now the condition of statistical stationarity as expressed within isentropic corrdinates requires the isentropically area average entropy source $\hat{\dot{s}}^{A_\theta}$ to vanish throughout the global domain. As such, with $\hat{\dot{s}}^{A_\theta}$ equal to zero throughout the climate state domain, the vertical deviation of $\hat{\dot{s}}^{A_\theta *}$ is identically zero. From a physical perspective, this condition simply requires the increase of entropy within each isentropic layer by solar absorption, sensible and latent heating plus frictional dissipation to be equal to the loss of entropy from the climate system by infrared emission. Now under these conditions, the impact of the cold bias on the model state reduces to

$$\begin{aligned} &\{\left\langle [\dot{s}^{***}(\varepsilon_{A_\theta} T)^{***} \right\rangle\} \\ &\quad = \{\left\langle \tilde{\dot{s}}^{***}(\tilde{\varepsilon}_{A_\theta} \tilde{T})^{***} \right\rangle\}[1-(\Delta \overline{T} / \overline{\tilde{T}}) \end{aligned} \qquad (50)$$

As the result reveals, when the internal energy distribution is expressed relative to the entropy structure as determined by casting the results determined for generalized coordinates in isentropic coordinates, the impact of the mean cold bias is to amplify the generation of the reversible component of total energy. Clearly the greatest amplification will occur where the positive and negative efficiencies are the largest, that is the upper troposphere of polar latitudes, and the lower troposphere of the atmosphere on all isentropic surfaces which intersect the earth’s surface. Such amplification will extend into the lower troposphere of the extratropical latitudes such as over the Southern Ocean, where the cold air draining from the Antarctic Continent is heated by sensible heat addition over an extremely intense circumpolar circulation surrounding the Antartic Continent..

Isentropic Efficiency Factor

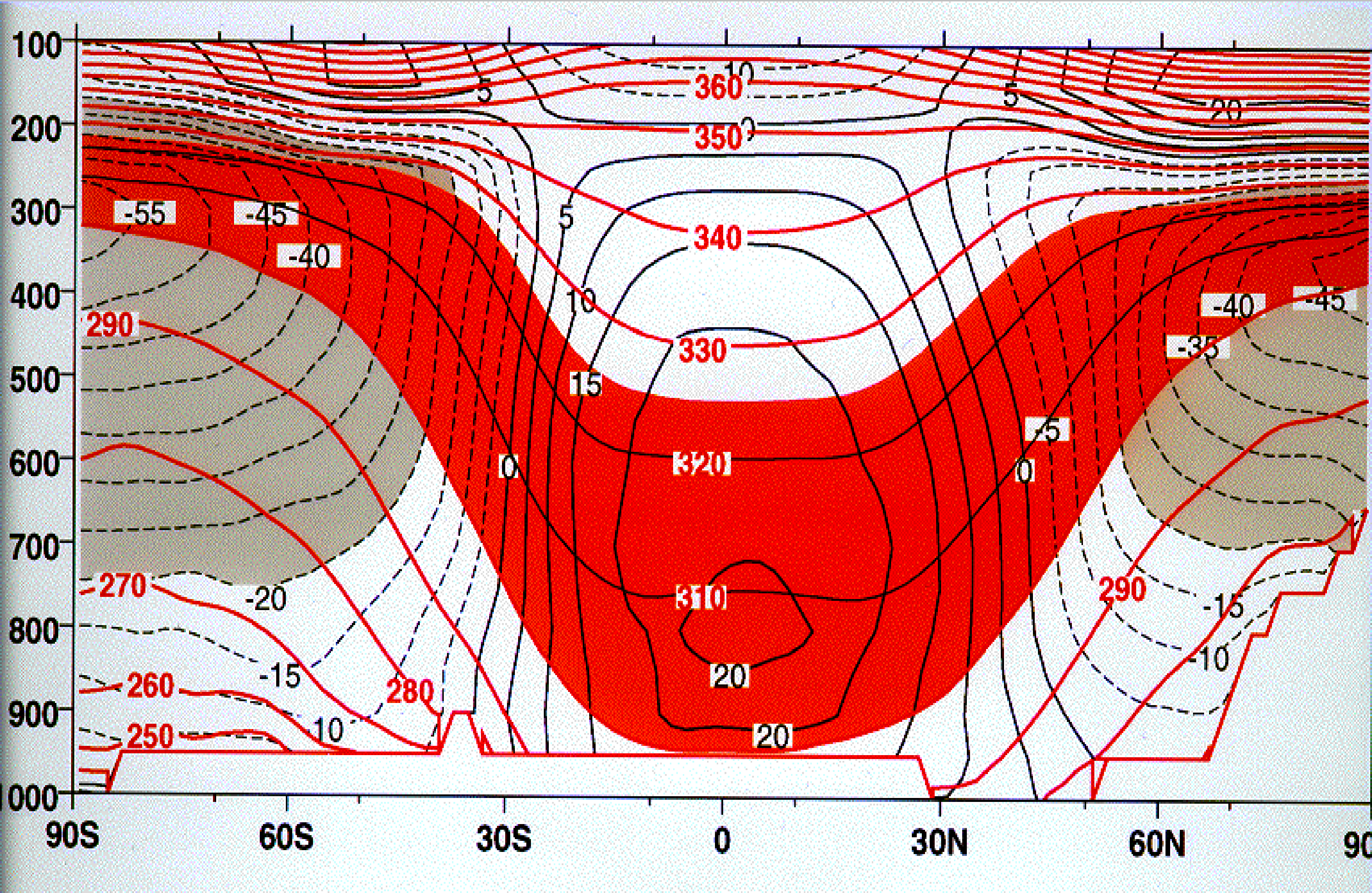

Air Temperature Differences

Mean Model

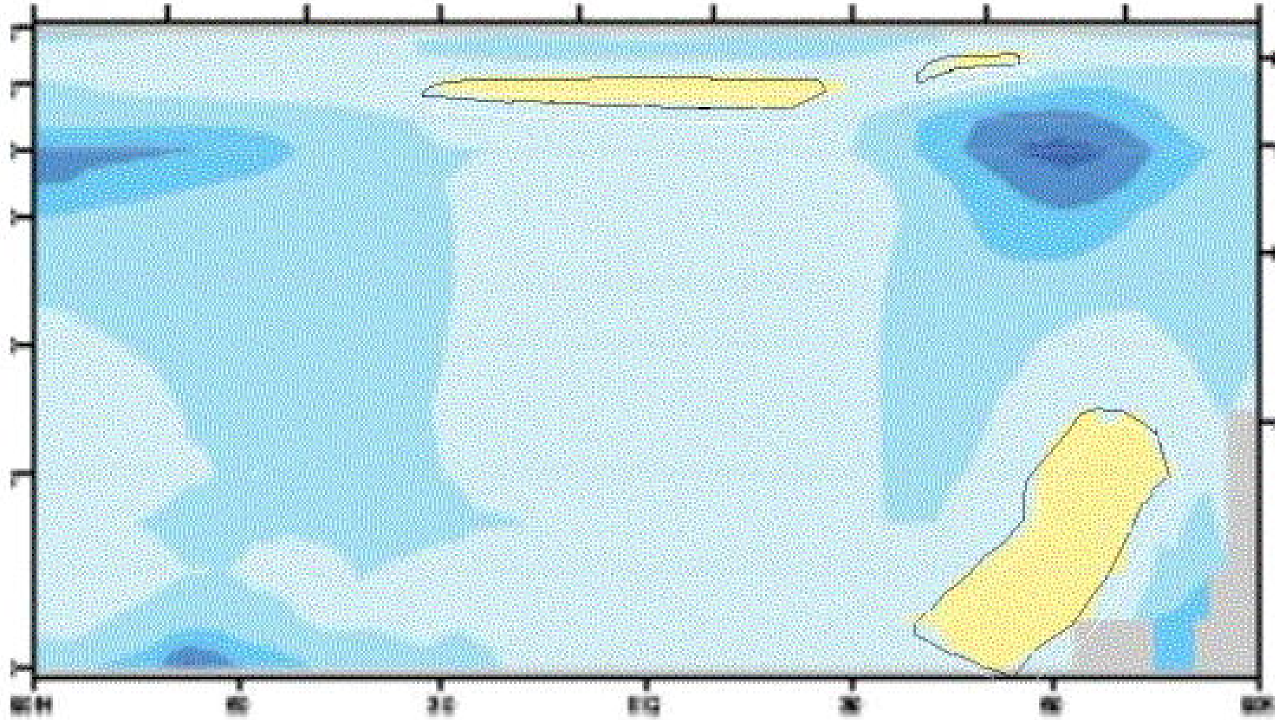

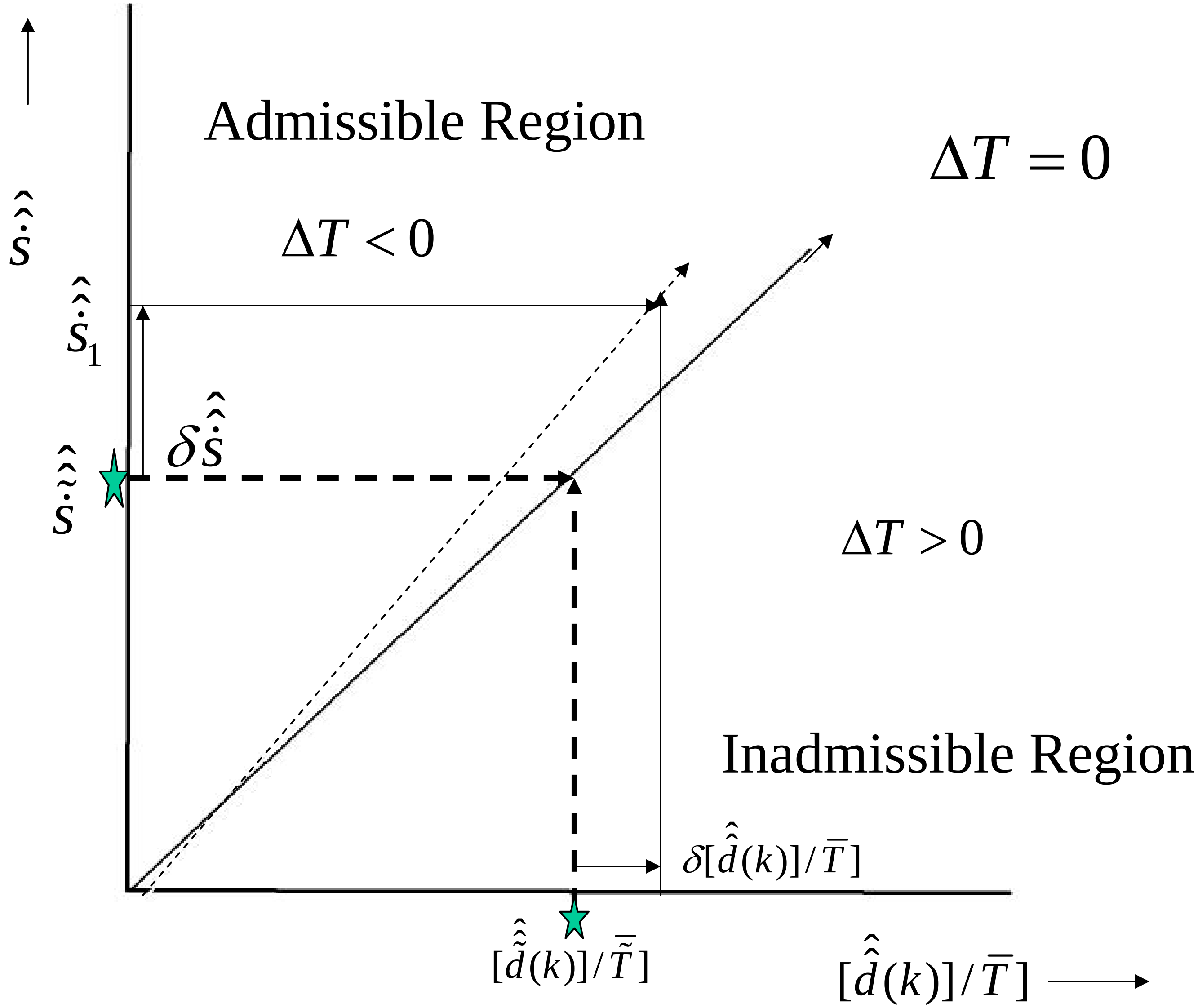

Within the relation $\hat{\dot{s}} = [\hat{\hat{d}}(k)/\tilde{\bar{T}}](1-(\Delta\bar{T}/\tilde{\bar{T}})]$ the quantity $[1-(\Delta\bar{T}/\tilde{\bar{T}})]$ defines the slope of the family of dashed lines as a function of the abscissa and the ordinate passing though the origin in relation to the mean cold bias .

Now compare the ratio of a model's mean entropy source to its kinetic energy dissipation to the true state ratio by the substitution of (14a) into (25), in the form of

$$[\hat{\hat{\dot{s}}} / \hat{\hat{d}}(k)] = [\hat{\hat{\tilde{\dot{s}}}} / \hat{\hat{\tilde{d}}}(k)](1-(\Delta\overline{T} / \overline{\tilde{T}})] > [\hat{\hat{\tilde{\dot{s}}}} / \hat{\hat{\tilde{d}}}(k)], \qquad (27)$$

and then note from (27) that a cold bias requires the ratio of the model's entropy source to its kinetic energy dissipation to be defined as R must be greater than the corresponding true state ratio to be defined as $\tilde{R}$.

Note that (27) may be expressed as

$$R = \tilde{R}\ (1-(\Delta\overline{T} / \overline{\tilde{T}})] > [\hat{\hat{\tilde{\dot{s}}}} / \hat{\hat{\tilde{d}}}(k)]$$

where R and $\tilde{R}$ are defined by $R = \hat{\hat{\dot{s}}} / \hat{\hat{d}}(k)$ and $\tilde{R} = \hat{\hat{\tilde{\dot{s}}}} / \hat{\hat{\tilde{d}}}(k)$

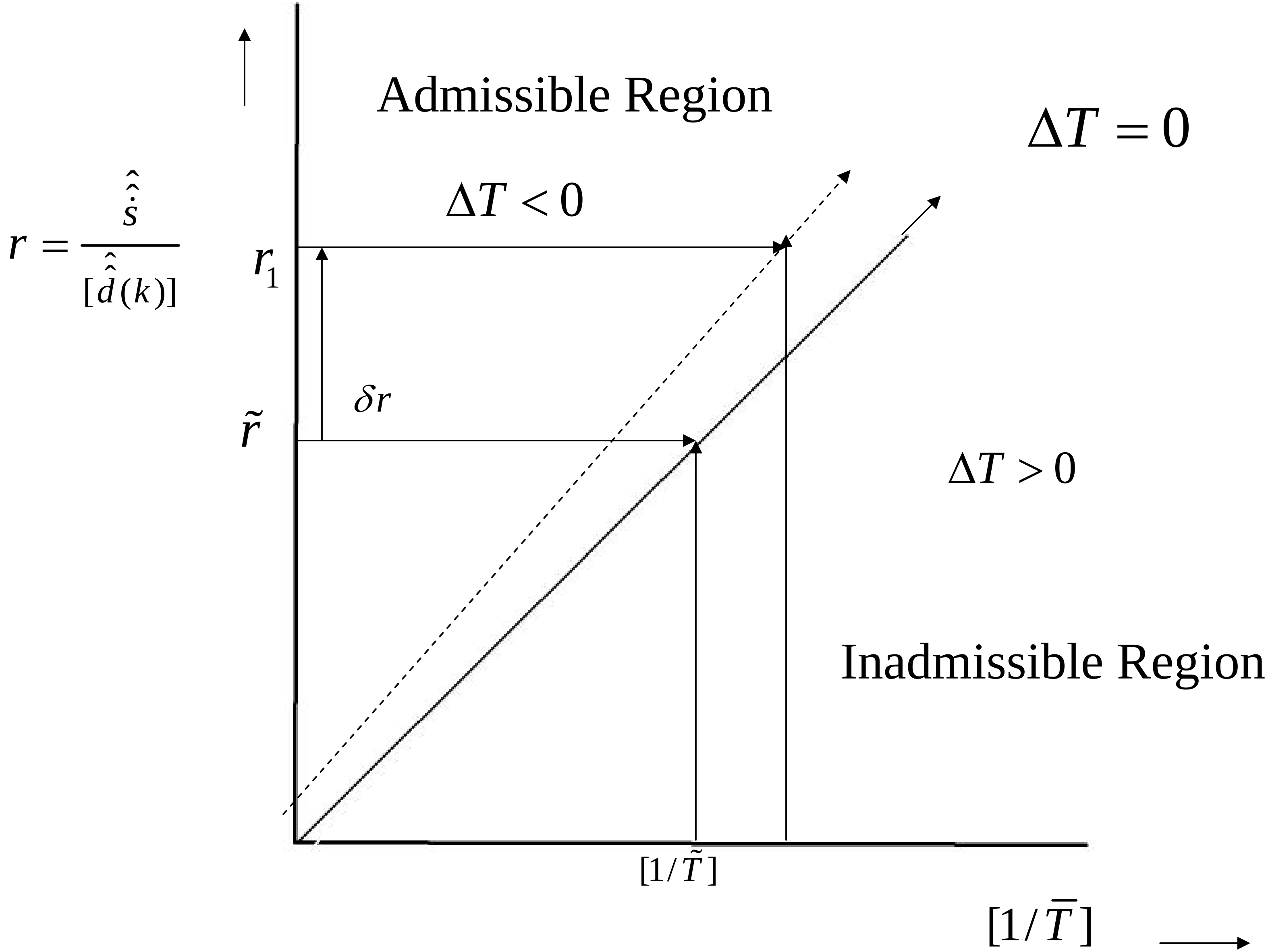

$[(1-(\Delta T/\bar{\tilde{T}})]$ defines the slope of the family of dashed lines as a function of the abscissa and the ordinate passing though the origin in relation to the mean cold bias ΔT .

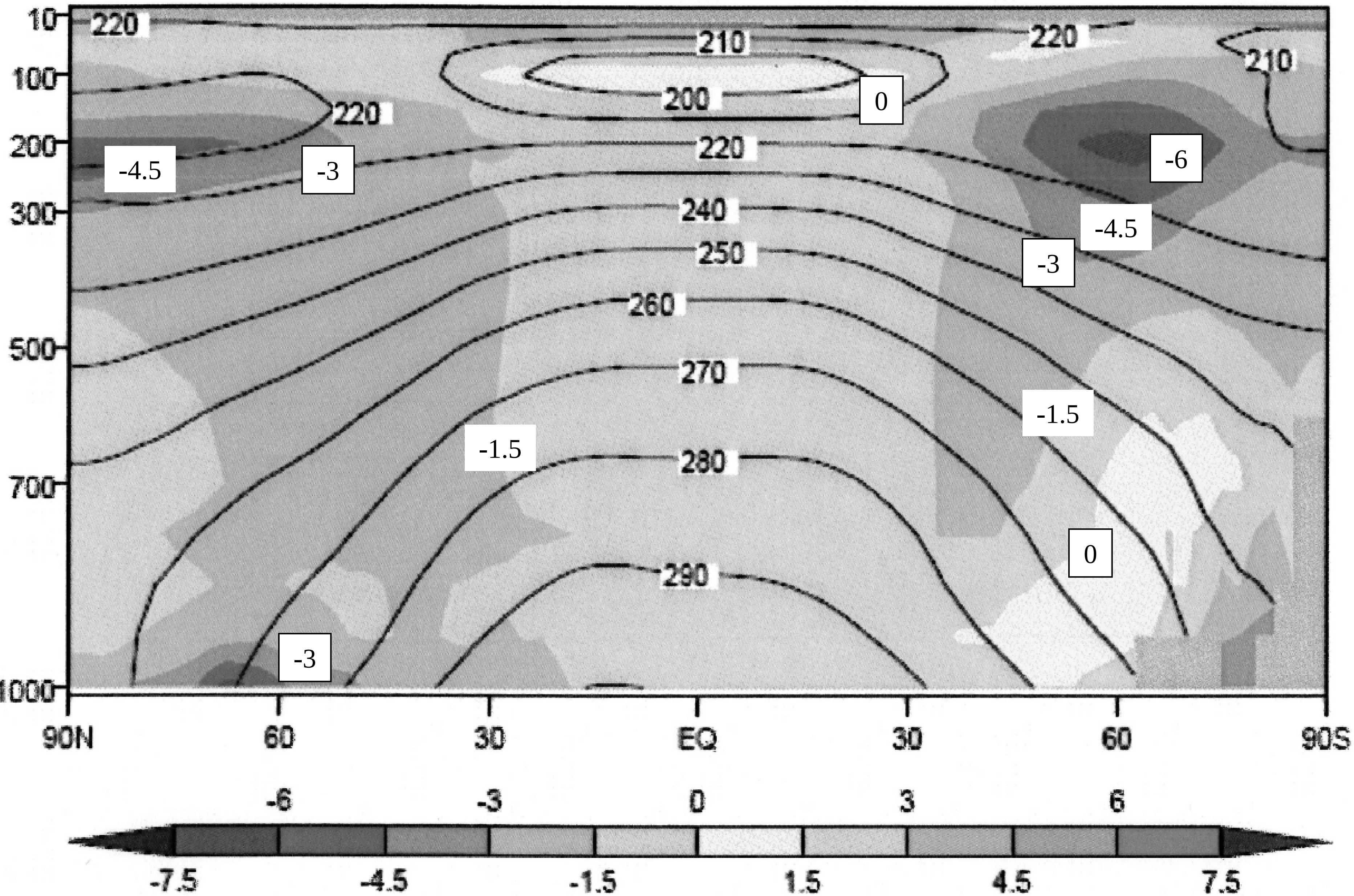

10
100
200
300
500
700
1000
90N
60
30
EQ
30
60
90S
220
210
200
220
240
250
260
270
280
290
220
220
210
0
-4.5
-3
-6
-4.5
-3
-1.5
-1.5
0
-3
-6
-3
0
3
6
-7.5
-4.5
-1.5
1.5
4.5
7.5

Scatter Plots of $\theta - \theta_0$

UW θ-η model with NCEP Physics

2.8125 lat – long

28 layers

CAM 3 (Eulerian Spectral)

T42 (~2.8 resolution)

26 layers

CAM3 (Finite Volume)

2 x 2.5 lat – long

26 layers

No Physics

All models used 15 Dec. 2004

initial conditions

Day 10

θ - θ_0

No Physics
Day 10

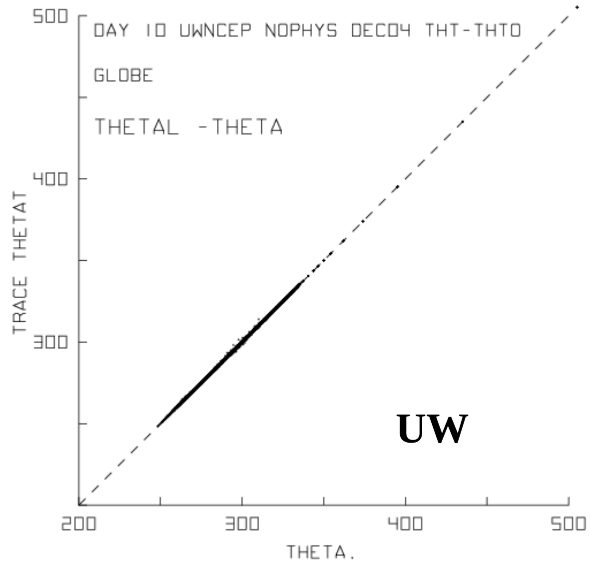

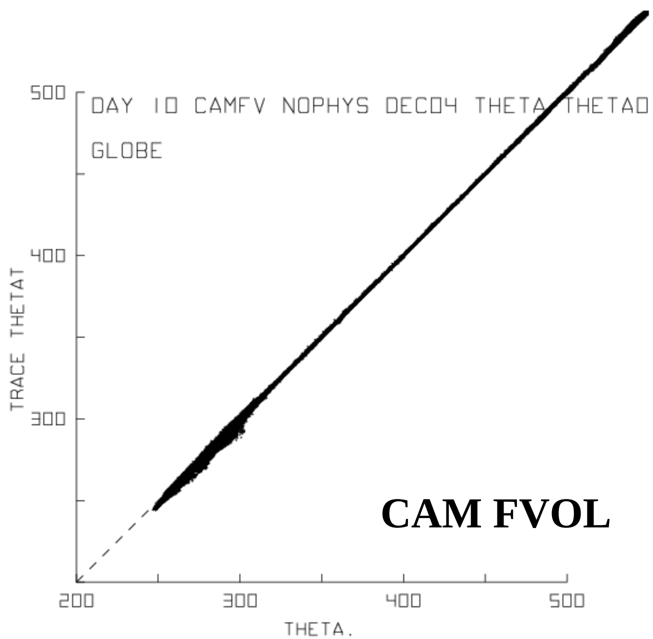

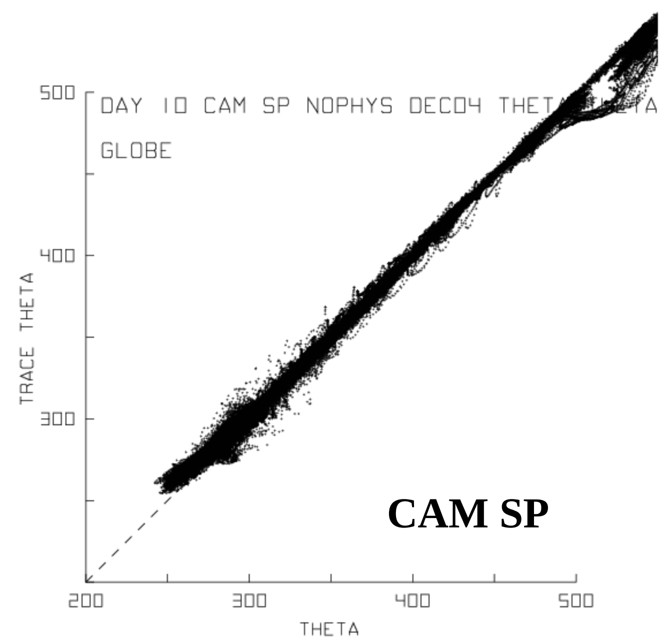

10 day Component Variance and RMS differences of Potential Temps- initial day 15 Dec. 1998,

	$(\theta_L - \theta_{L0})$	$(\theta - \theta_o)$	$(\theta_L - \theta)$	$(\theta_o - \theta_{L0})$
UW θ-η Model, 14 theta, 14 eta layer, 2.8125 deg				
CCM3 NO PHYS	1.12 (1.06)	0.02 (0.14)	0.28 (0.53)	0.28 (0.53)
CCM3 ALL PHYS	130.52 (11.43)	115.37 (10.74)	1.79 (1.34)	1.82 (1.35)
NCAR FV 26 layers, 2x2.5 deg				
CAM3 NOPHYS	6.93 (2.63)	1.00 (1.00)	1.54 (1.24)	1.53 (1.24)
CAM3 ALL PHYS	210.97 (14.53)	156.99 (12.53)	6.52 (2.55)	6.18 (2.49)

30 day Component Variance and RMS differences of Potential Temps- initial day 15 Dec. 1998,

UW Model, CCM3 All Physics, 14 theta, 14 eta layer, 2.8125 deg

	$(\theta_L - \theta_{L0})$	$(\theta - \theta_o)$	$(\theta_L - \theta)$	$(\theta_o - \theta_{L0})$
UW θ-η Model	477.52 (21.85)	402.89 (20.07)	8.27 (2.88)	9.17 (3.03)
UW Sigma Model	1752.90 (41.87)	661.55 (25.72)	181.95 (13.49)	118.11 (10.87)

Temperature Tracer on 300 K Topography Viewed from 90E

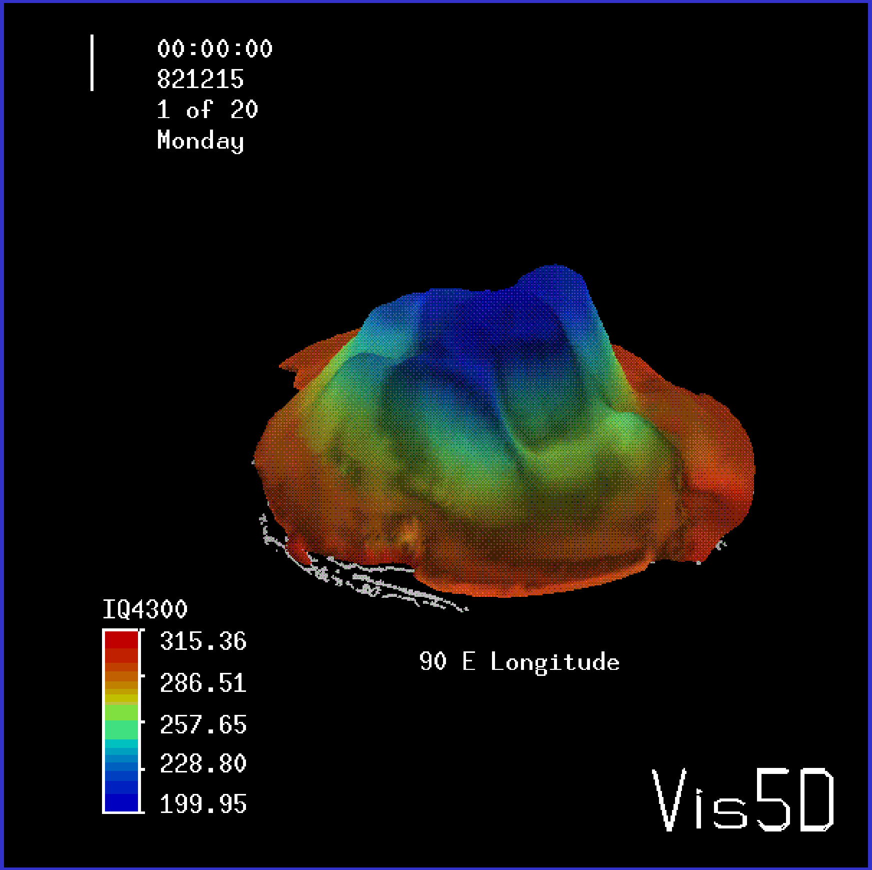

5 Day Simulation of 292 K Specific Humidity Superimposed on 292 K Pressure Topography

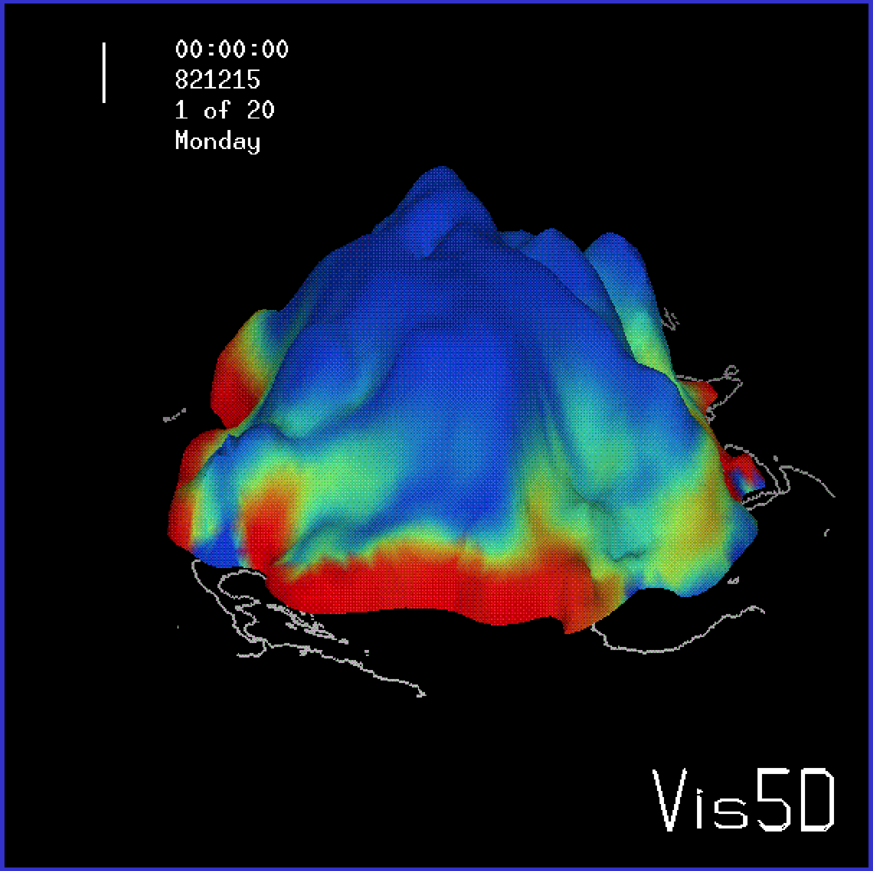

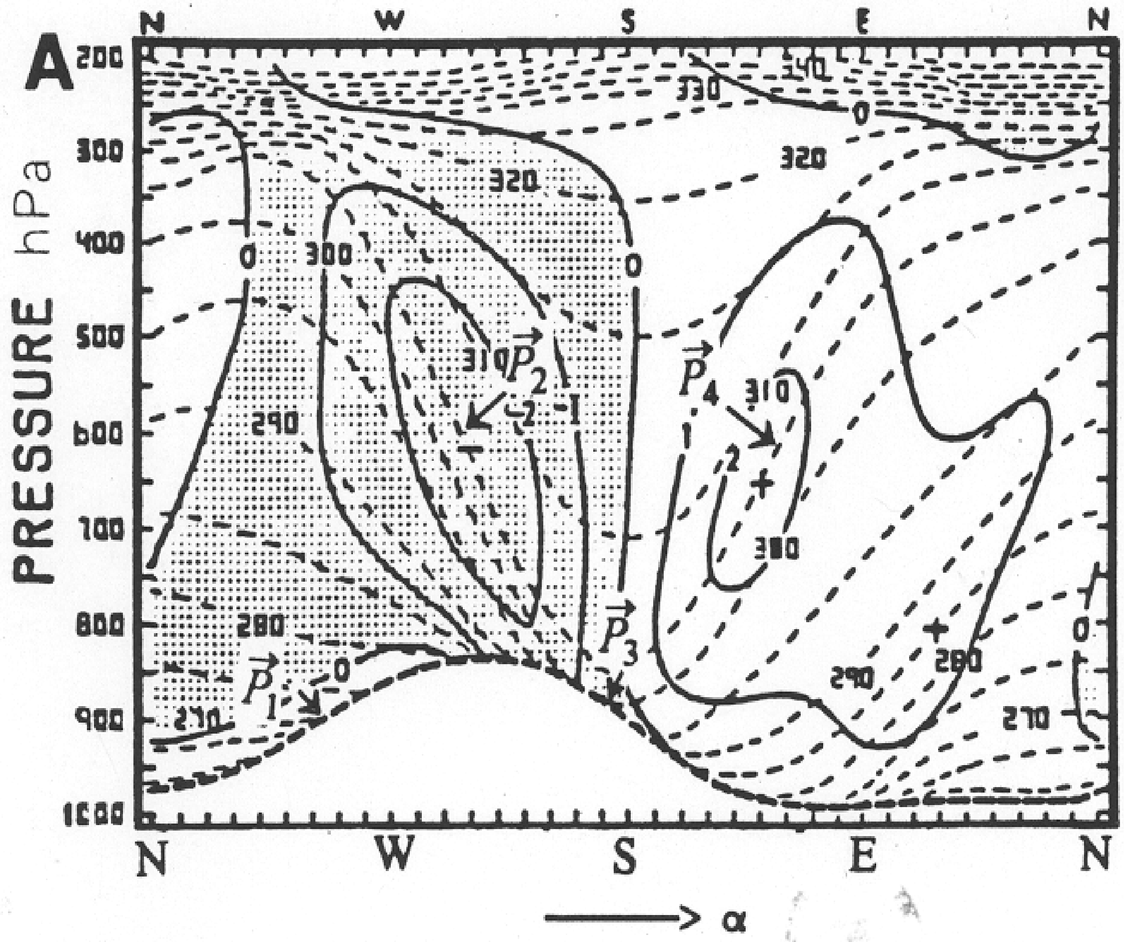

Fig. 13. Vertical–azimuthal distribution of azimuthal component of pressure stress on isentropic surfaces (solid) and potential temperature (dashed) for the radius of 9.0° within the Alberta cyclone at 1200 UTC 31 March 1971 (10^8 kg s^{-2}) (Katzfey, 1978). The cyclonic rotation (α) goes from the north (N) to the west (W), to the south (S), to the east (E) and back to the north.

NCAR CCM3

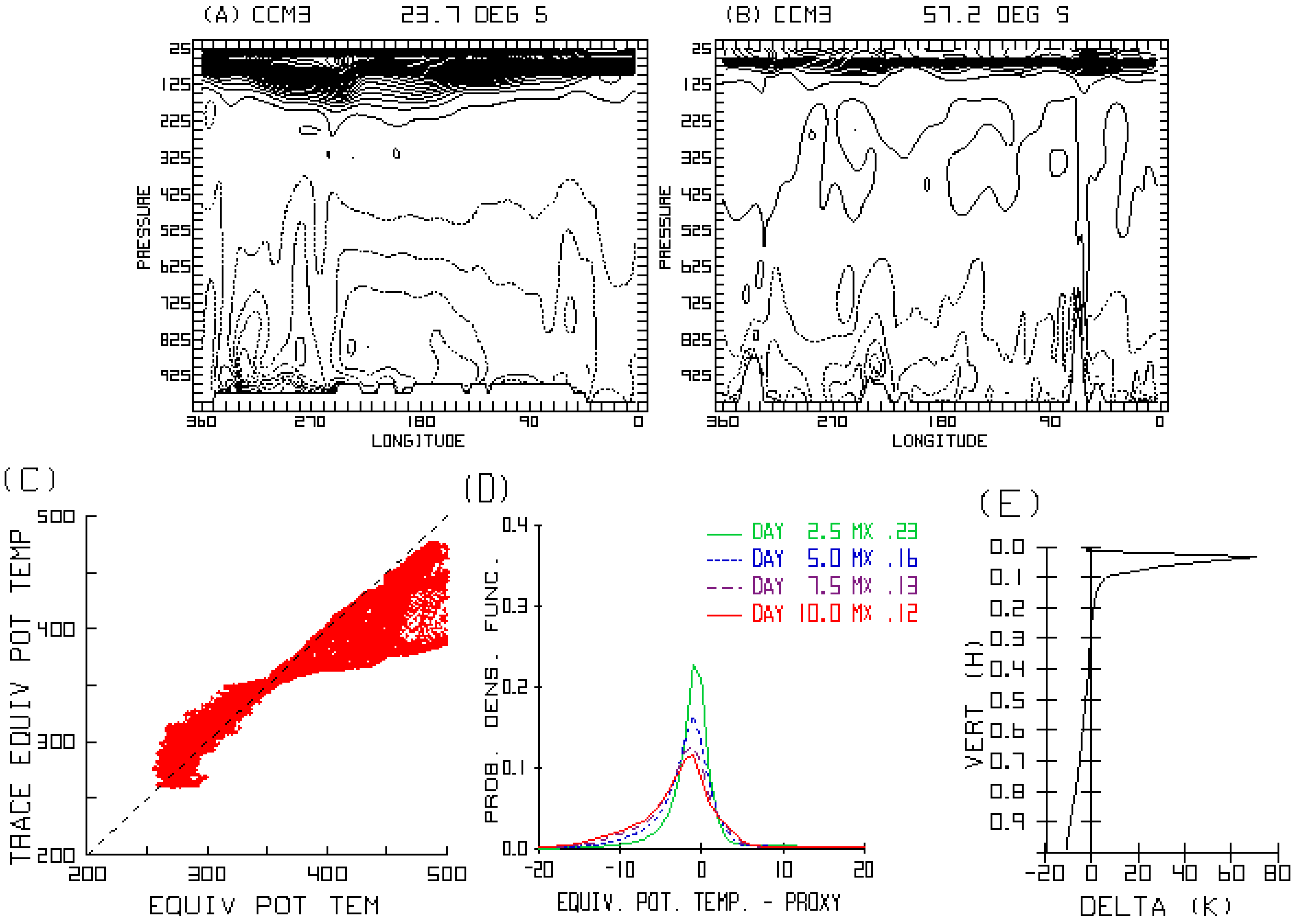

(A) CCM3 23.7 DEG S
(B) CCM3 57.2 DEG S
PRESSURE
25
125
225
325
425
525
625
725
825
925
360
270
180
90
0
LONGITUDE
(C)
TRACE EQUIV POT TEMP
EQUIV POT TEM
200
300
400
500
(D)
PROB. DENS. FUNC.
0.0
0.1
0.2
0.3
0.4
DAY 2.5 MX .23
DAY 5.0 MX .16
DAY 7.5 MX .13
DAY 10.0 MX .12
-20
-10
0
10
20
EQUIV. POT. TEMP. - PROXY
(E)
VERT (H)
0.0
0.1
0.2
0.3
0.4
0.5
0.6
0.7
0.8
0.9
-20
0
20
40
60
80
DELTA (K)

UW Hybrid θ-η Model

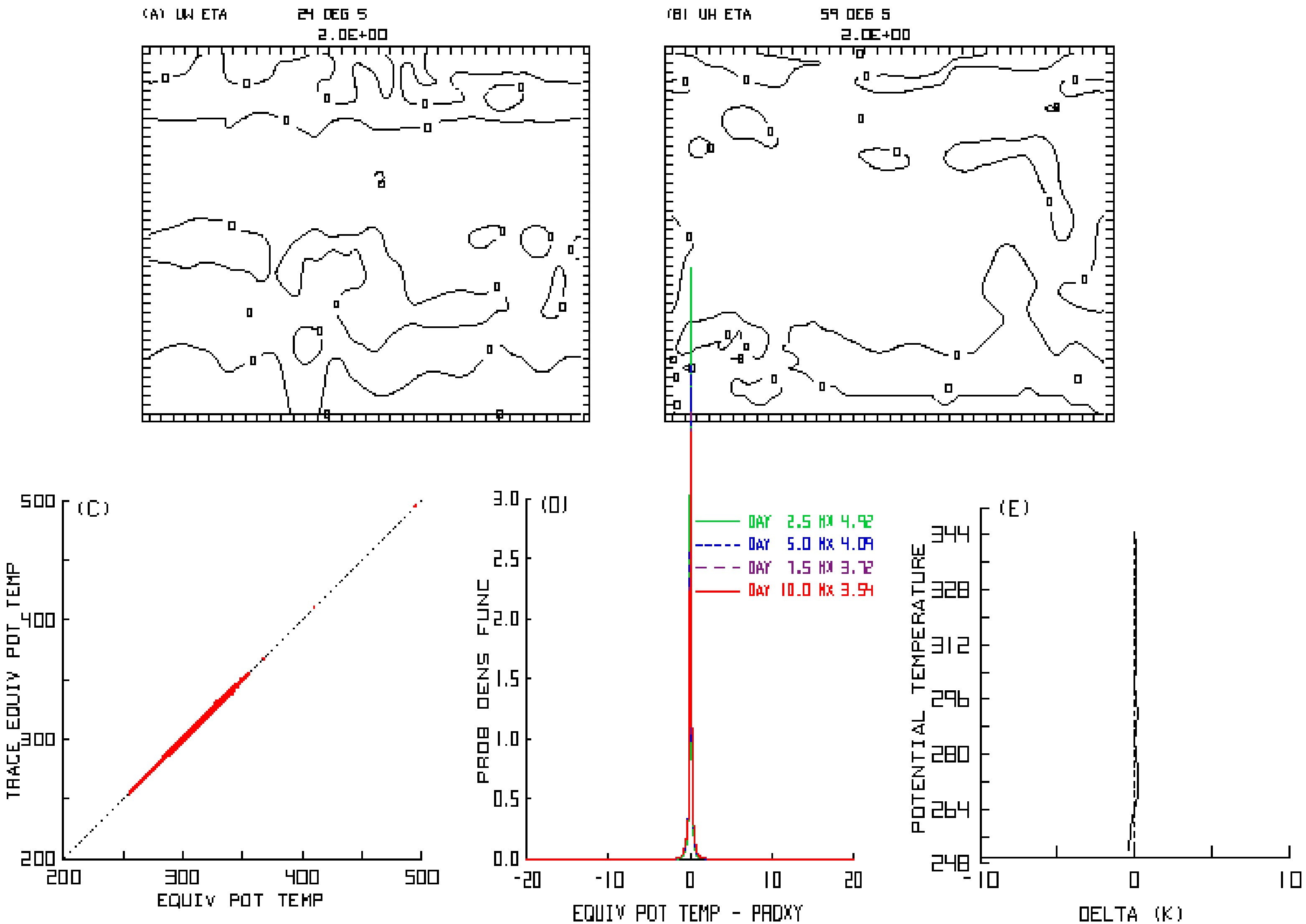

Zonally Averaged Water Vapor Transport

January 1979

GLA Assimilated Data

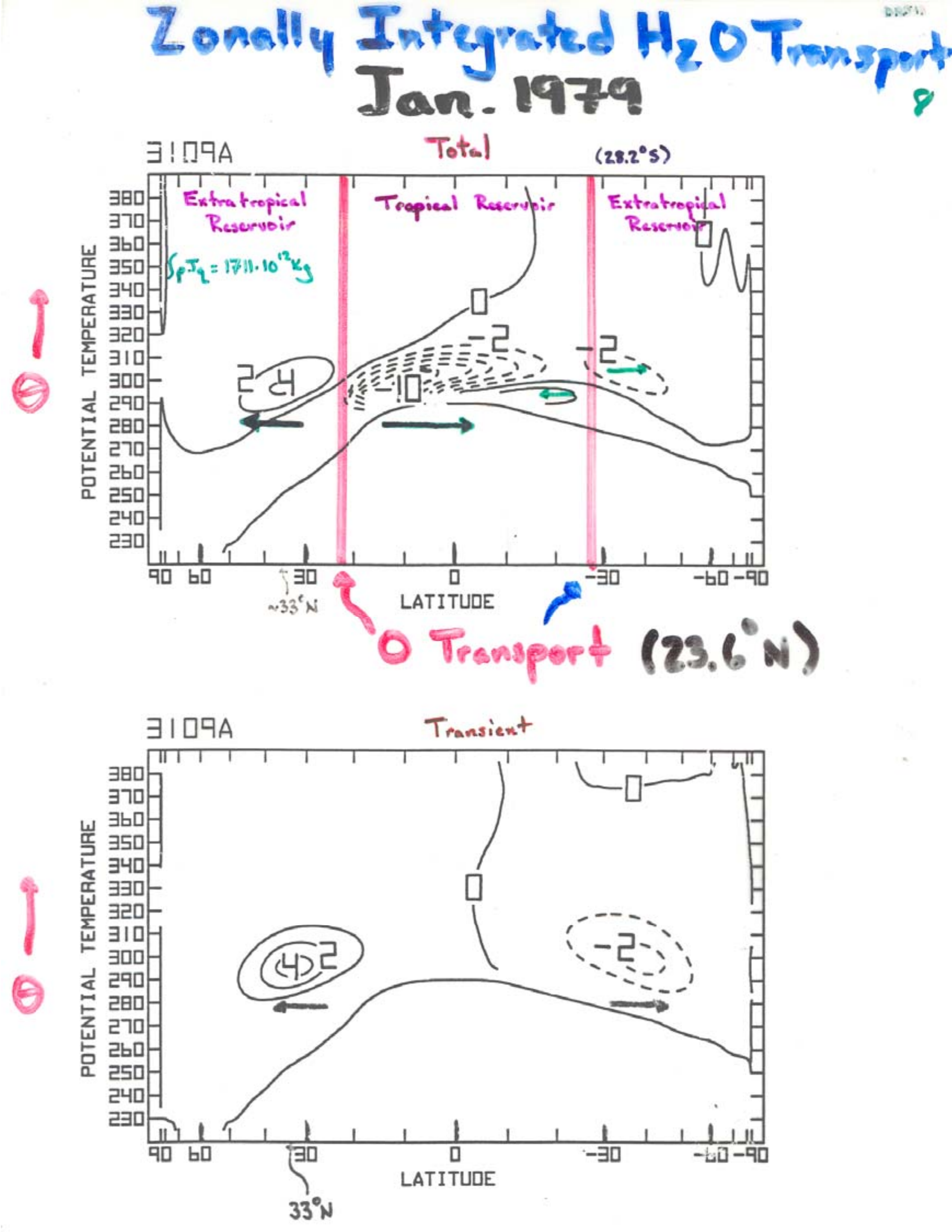

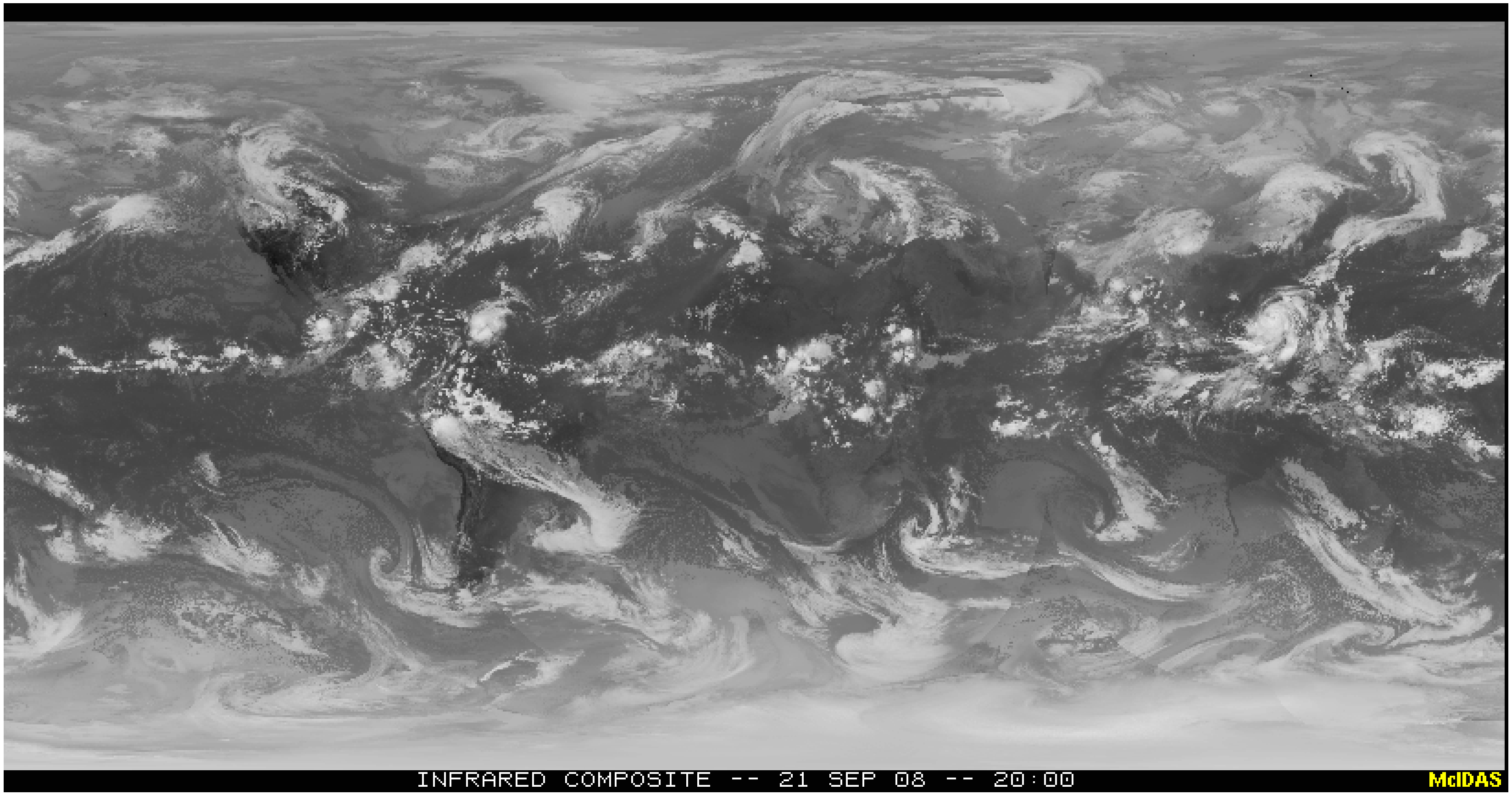
INFRARED COMPOSITE -- 21 SEP 08 -- 20:00
McIDAS

The End

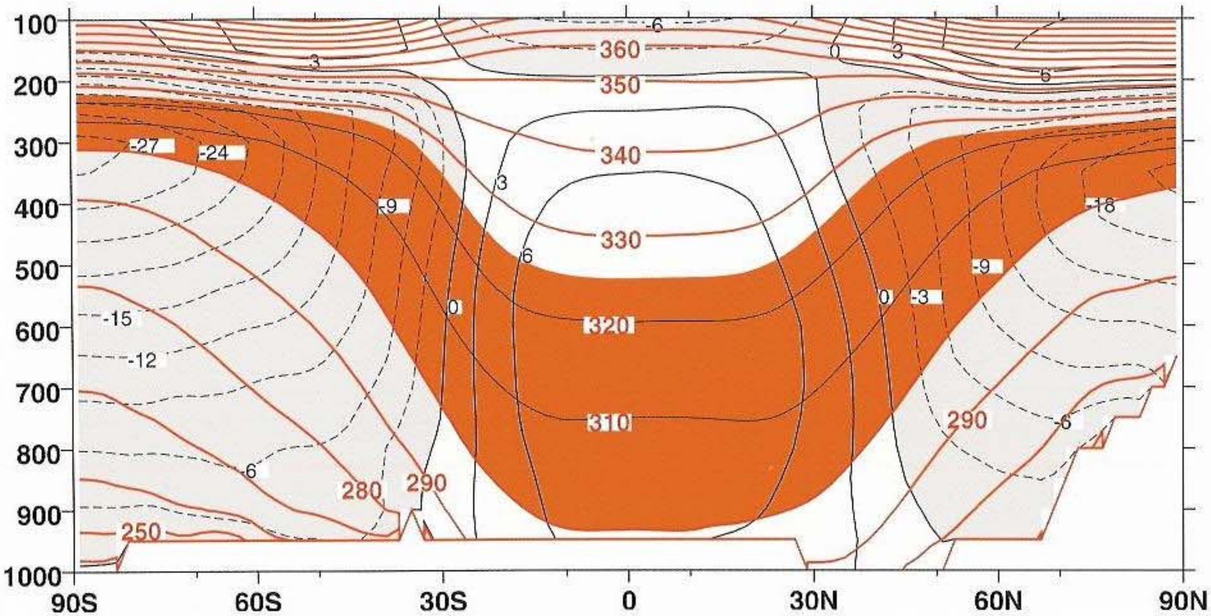

Figure 22.2 A vertical meridional distribution of mass weighted temporally, zonally averaged isentropic efficiency (units 10^{-2}) defined by $\hat{\varepsilon}$ equal to $< (1-T_\alpha/T) >$ [see Eq. (44)] and potential temperature $\theta[\phi, \overline{p}^{\lambda,t}(\phi,\theta)]$ (K) as determined from the isentropic temporally, zonally averaged pressure distribution, $\overline{p}^{\lambda,t}(\phi,\theta)$. Unshaded and shaded regions denote positive and negative efficiencies., respectively. The isentropic layers shaded red identify the atmospheric region within which the covariance of entropy sources and sinks with positive and negative efficiencies, respectively, are most effective in the generation for maintaining the atmosphere's circulation. The nonlinearity of this process is evident from the consideration that a cooling rate of 1 K day^{-1} in the high polar troposphere with $\varepsilon < 0.25$ is four times as effective in generation as a heating rate of 1 K day^{-1} in the low to mid tropical troposphere with $\varepsilon \approx 0.06$. Alternatively, the nondimensional efficiencies as indicated may be considered to be percentages of the heating/cooling that generates a reversible component. For example, in high polar troposphere in the northern hemisphere, the generation contribution εQ_m means that 27% of the cooling rate with $Q_m < 0$ and $\varepsilon < 0$ is a positive generation contribution to the reversible component equal to 27% of $|Q_m|$.

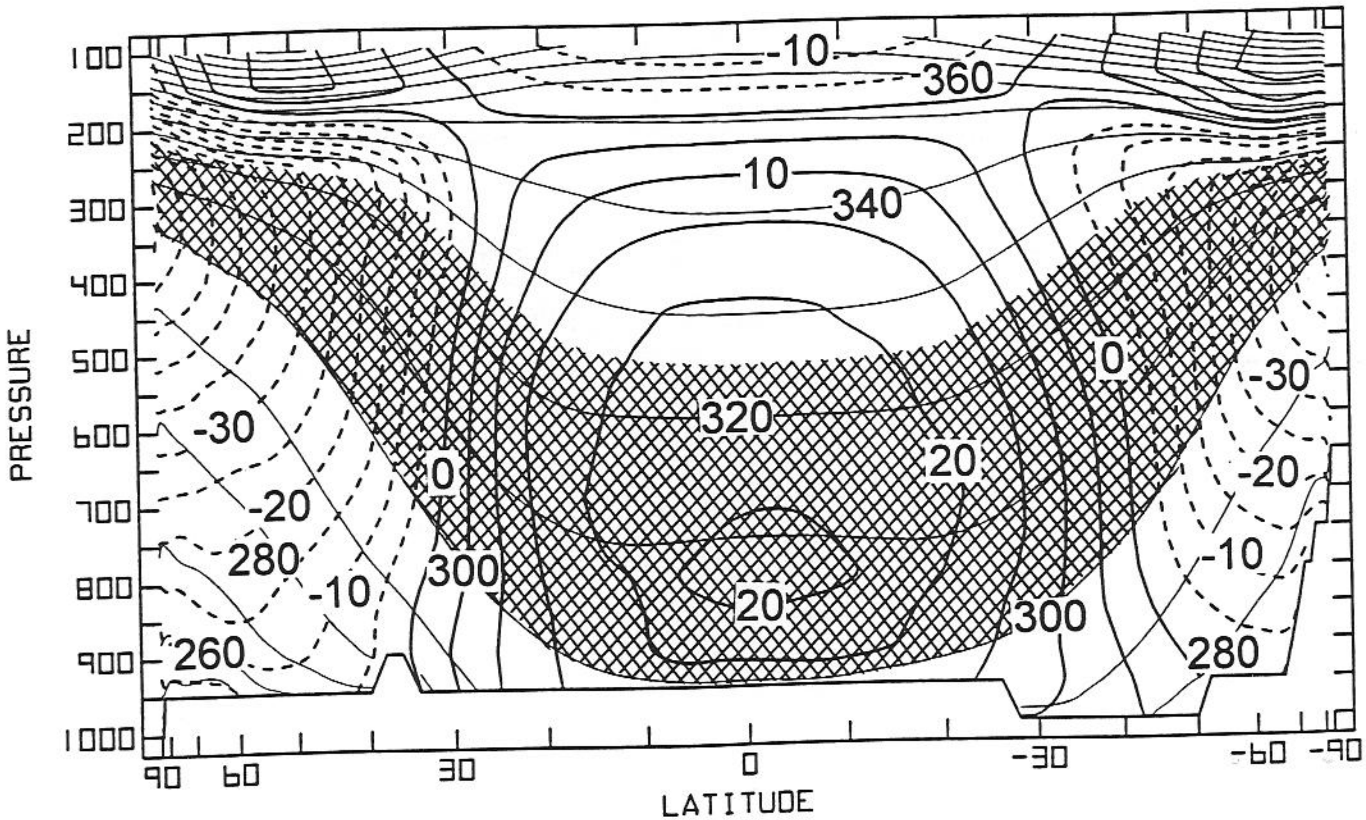

Figure 2: A reprsentative vertical meridional distribution of potential temperature $\theta[\phi,\overline{p}^{\lambda,t}(\phi,\theta)]$ as determined from the isentropic temporally, zonally averaged pressure distribution $\overline{p}^{\lambda,t}(\phi,\theta)$, and the corresponding isentropic zonally averaged departure temperature $\overline{\Delta T}^{\lambda,t} = \overline{T(\phi,\theta)-T_{\alpha}(\theta)}^{\lambda,t}$ where $T(\phi,\theta)=\theta[\overline{p}^{\lambda,t}(\phi,\theta)/p_{oo}]^{\kappa}$ and $T_{\alpha}(\theta)=\theta[\overline{p}^{\lambda,\phi,t}(\theta)/p_{oo}]^{\kappa}$ for Jan. 1-14, 1987.

A Reviewers Comment

It is doubtful that strict global conservation of energy and entropy by a numerical scheme plays a significant role in weather prediction. The advantage of center difference schemes like Arakawa and Lamb (1977) in conserving energy and entropy are often over-stated while its shortcomings (e.g., numerical instability near poles; degradation in vorticity advection in divergent flows which results in poor correlation between potential vorticity and passive tracers) being ignored. All models need sub-grid damping mechanisms. How this can be achieved can be very different among models. It should be noted that even the Arakawa and Lamb scheme needs artificial smoothing/filtering (in time and in space) renders all GCMs effectively non-energy conserving and irreversible. In standard CCM3 the total energy is nearly conserved because, 1) the lost kinetic energy due to hyper-viscosity is added back to the thermodynamic equation and also due in part, 2) a lucky cancellation between the energy conserving errors in dynamics and physics.

GFS Cold Bias

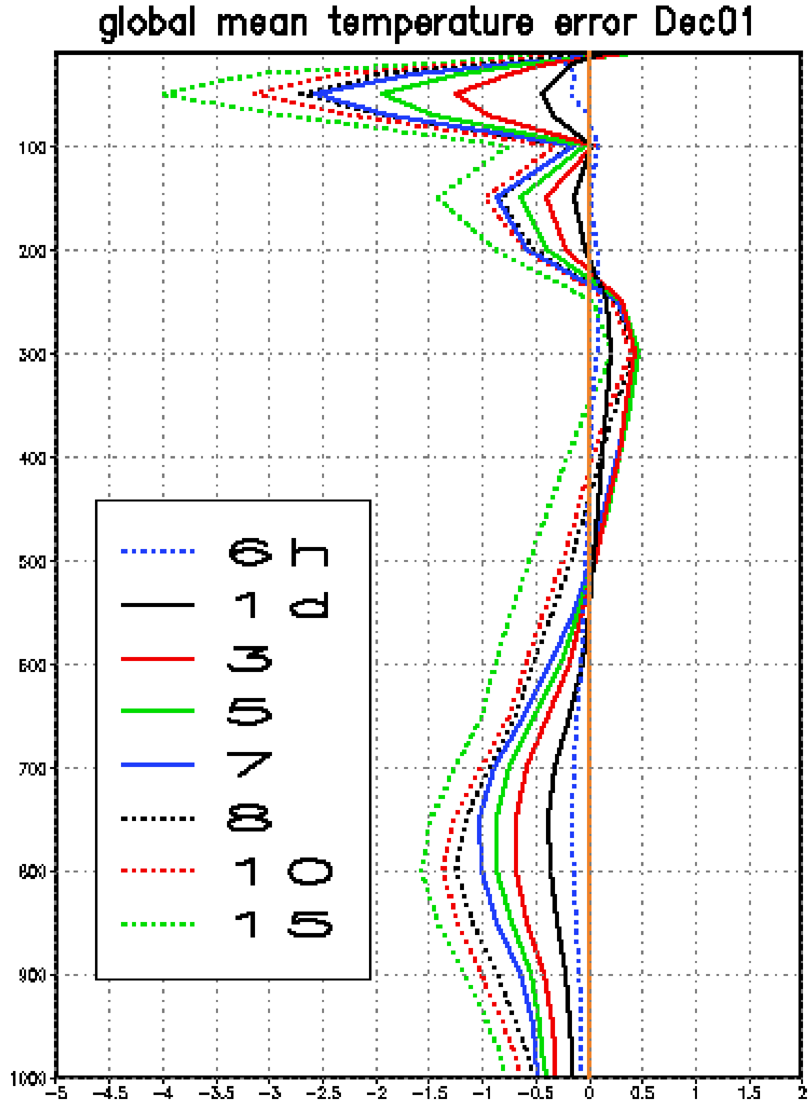

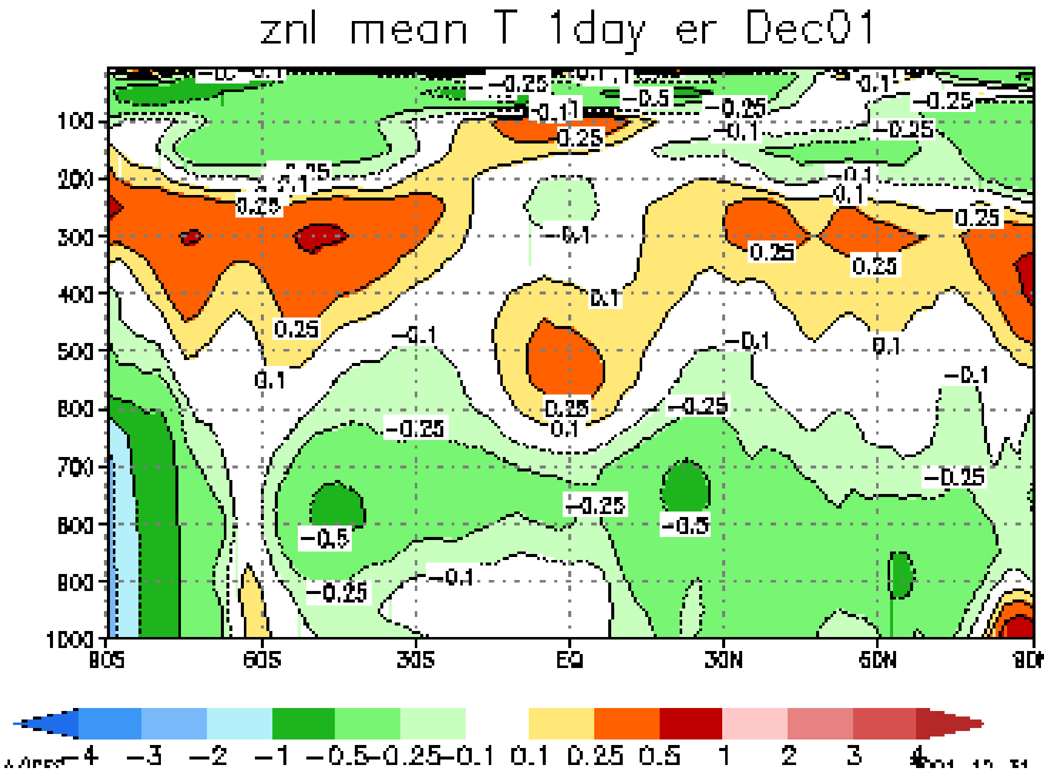

$$T^{***} = [(T - T_{e_{A_\theta}})^{***} + (T_{e_{A_\theta}} - \hat{T}^{A_\eta})^{***}] + (\hat{T}^{A_\eta} - \hat{T}^{G})^{*}$$

The Extended Proportion Defining *Carathéodory's Admissible Surfaces* *

$$\theta_\ell : \theta_o = (c_1 T_\ell^{1-\kappa} \alpha_\ell^{\kappa}) : (c_1 T_o^{1-\kappa} \alpha_o^{\kappa}) = (c_2 T_\ell / p_\ell^{\kappa}) : (c_2 T_o / p_o^{\kappa})] = (c_3 \alpha_\ell p_\ell^{1-\kappa}) : (c_3 \alpha_o p_o^{1-\kappa}) = (\theta / \theta_{\ell_o})$$

Carathéodory's Two Dimensional Surface as a function of (α, T, θ)

$$\sigma_{o1} = \sigma_1 = \frac{c_1 (T^{1-\kappa} \alpha^{\kappa})}{\theta_\ell} = \frac{c_1 \lambda_1}{\theta_\ell} = \frac{\theta(c_1, T, \alpha)}{\theta_\ell} = \frac{\theta_{\ell_o}(c_1, T_o, \alpha_0)}{\theta_o}$$

$$c_1 = (p_{oo} / R)^{\kappa}$$

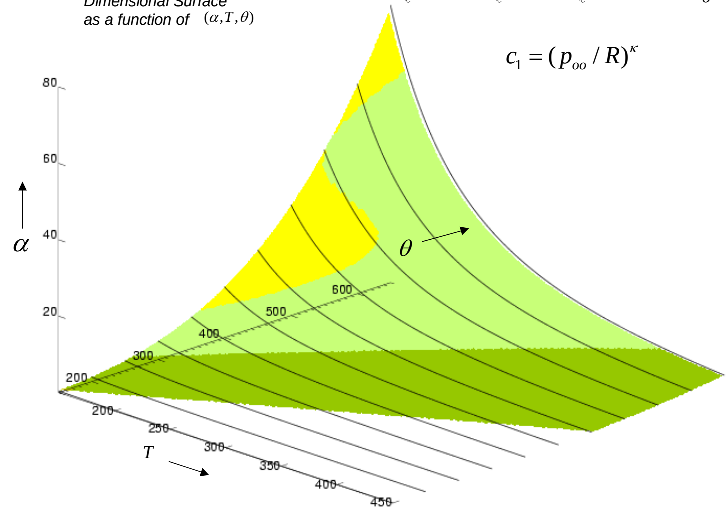

Carathéodory's Two Dimensional Surface as a function of (T, p, θ)

$$\sigma_{o2} = \sigma_2 = \frac{c_2 (T / p^{\kappa})}{\theta_\ell} = \frac{c_2 \lambda_2}{\theta_\ell} = \frac{\theta(c_2, T, p^{\kappa})}{\theta_\ell} = \frac{\theta_{\ell_o}(c_2, T_o, p_o^{\kappa})}{\theta_o}$$

$$c_2 = (p_{oo}^{\kappa})$$

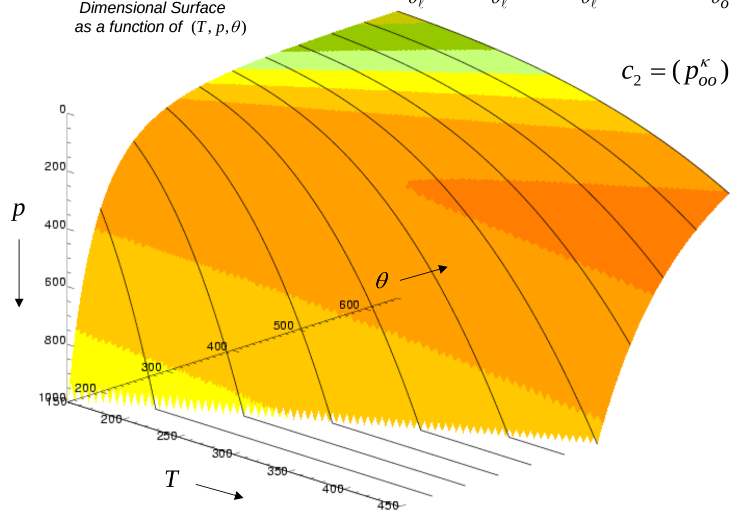

Carathéodory's Two Dimensional Surface as a function of (α, p, θ_ℓ)

$$\sigma_{o3} = \sigma_3 = \frac{c_3 (\alpha\, p^{1-\kappa})}{\theta_\ell} = \frac{c_3 \lambda_3}{\theta_\ell} = \frac{\theta(c_3, \alpha, p^{1-\kappa})}{\theta_\ell} = \frac{\theta_{\ell_o}(c_2, \alpha_o, p_o^{1-\kappa})}{\theta_o}$$

$$c_3 = (p_{oo}^{\kappa} / R)$$

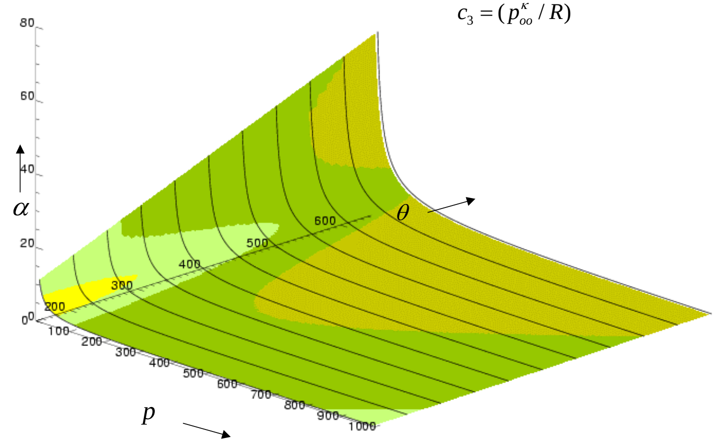

The Two Dimensional surface For the Ideal Gas Law

$$R = (p\alpha / T)$$

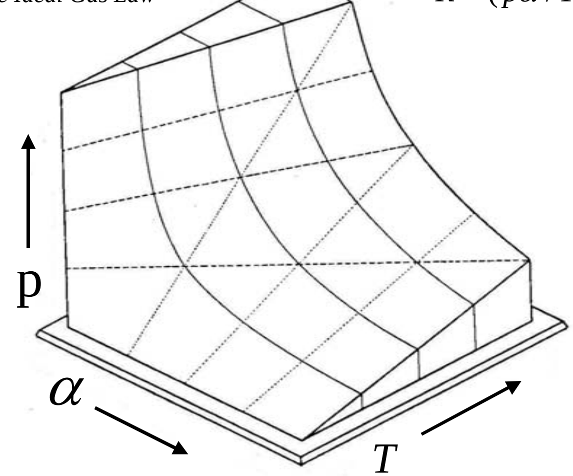

* Extracted from manuscript in preparation, Johnson (2007)

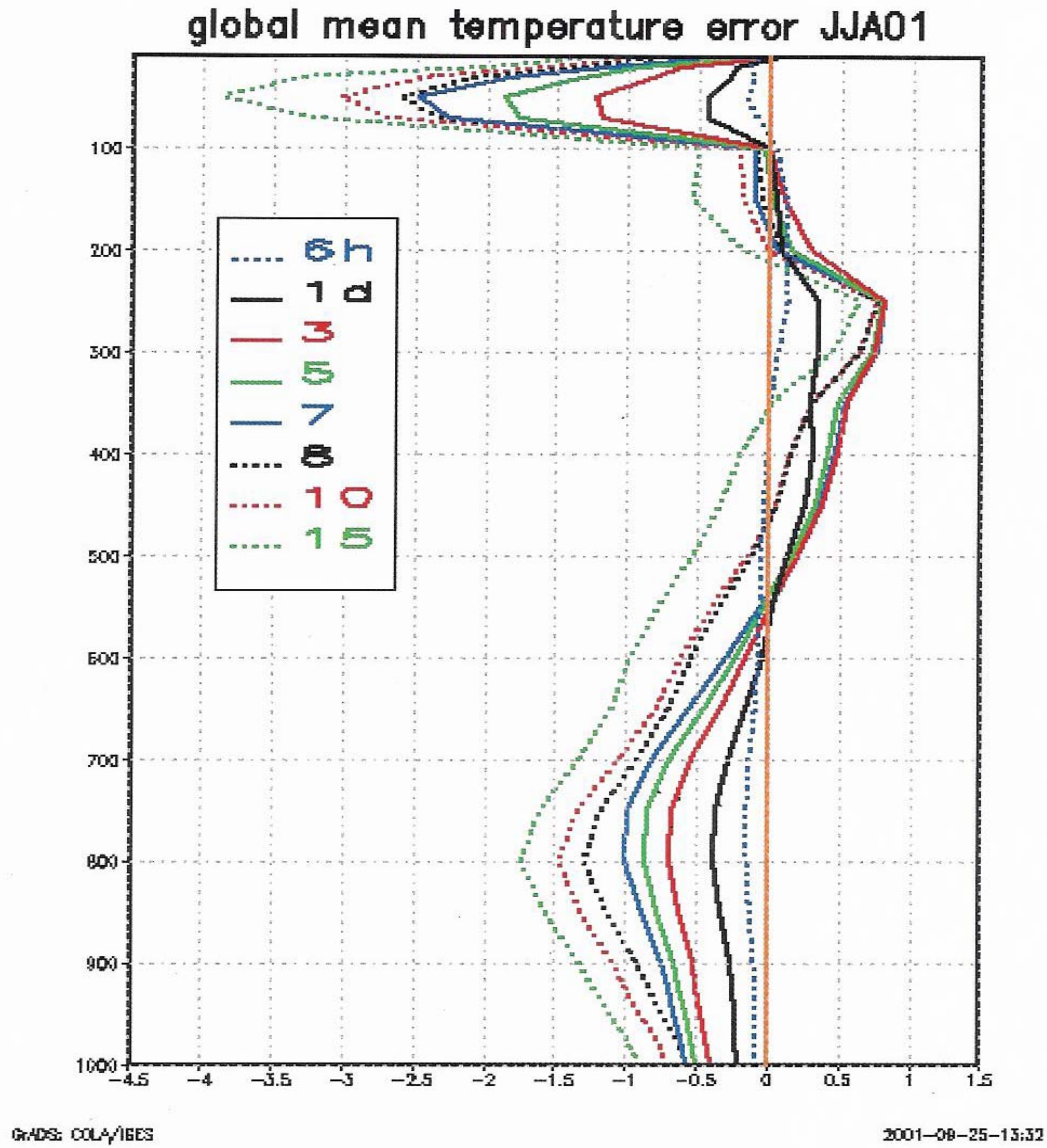

global mean temperature error JJA01
6h
1d
3
5
7
8
10
15
100
200
300
400
500
600
700
800
900
1000
-4.5
-4
-3.5
-3
-2.5
-2
-1.5
-1
-0.5
0
0.5
1
1.5
GrADS: COLA/IGES
2001-09-25-13:32

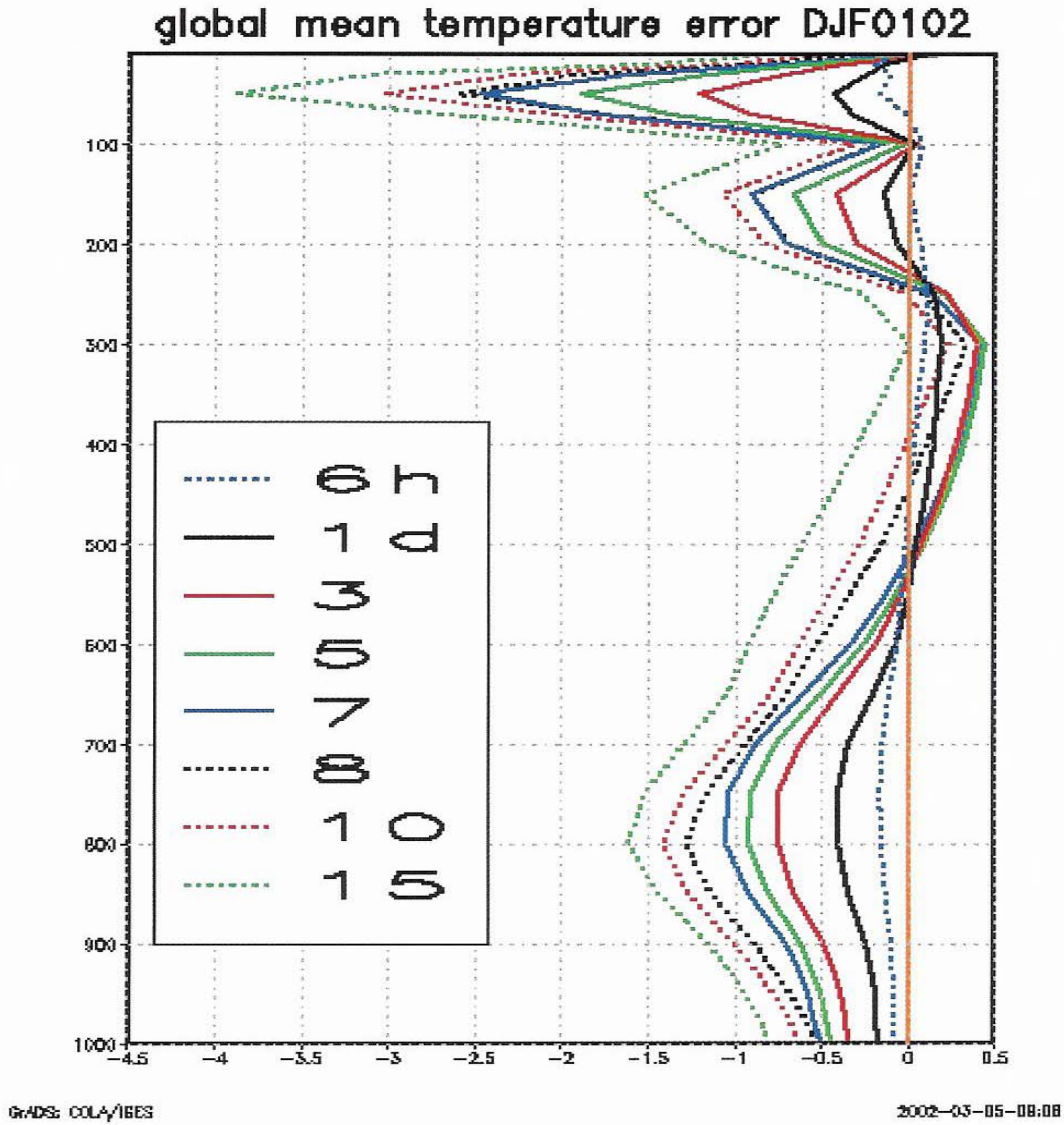

global mean temperature error DJF0102
100
200
300
400
500
600
700
800
900
1000
-4.5
-4
-3.5
-3
-2.5
-2
-1.5
-1
-0.5
0
0.5
6 h
1 d
3
5
7
8
10
15
GrADS: COLA/IGES
2002-03-05-09:08

θ - θ_0

No Physics
Day 10

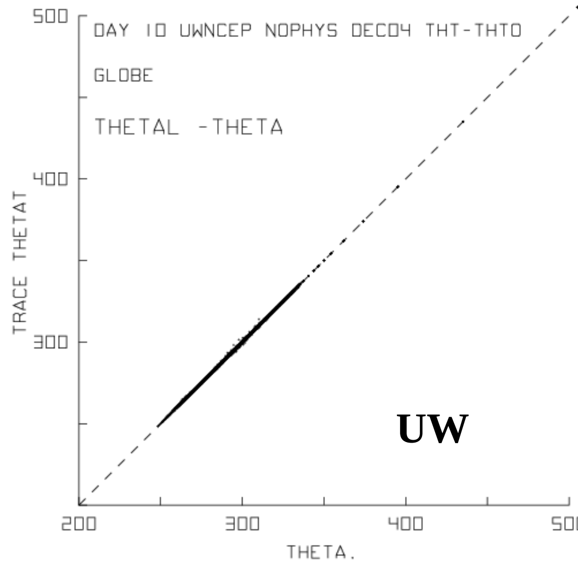

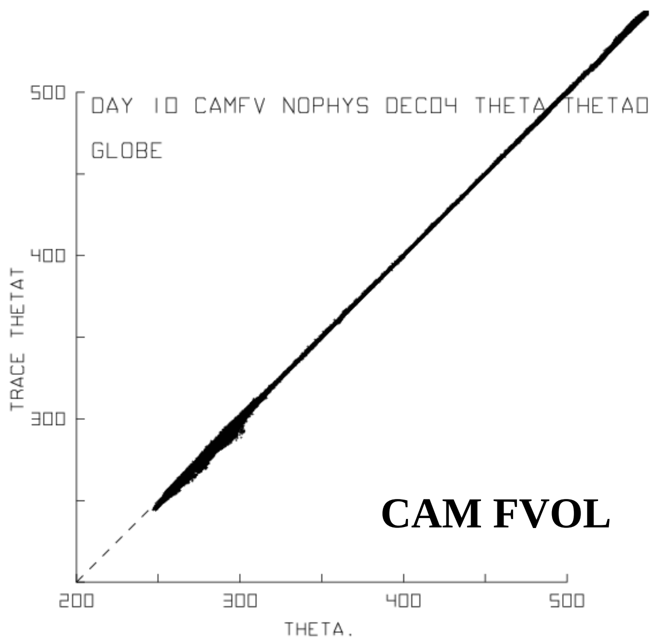

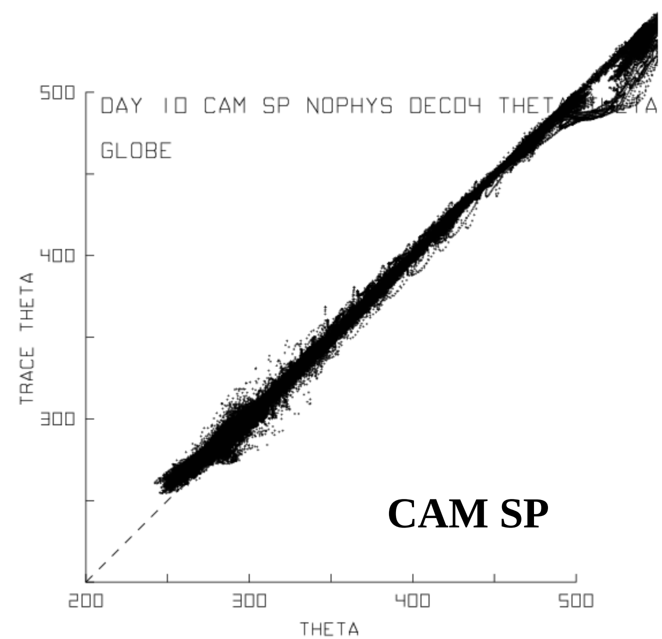

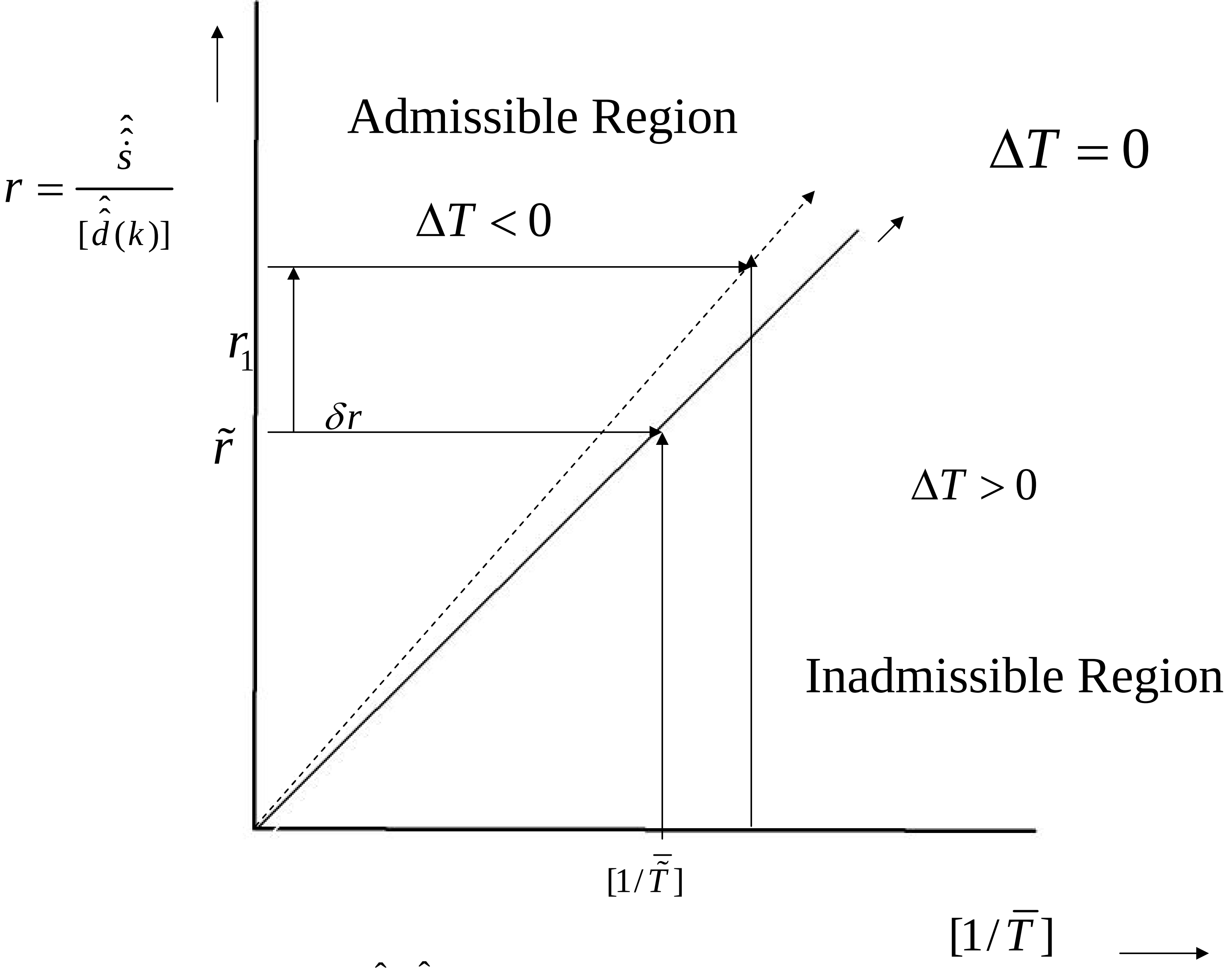

$[\bar{\tilde{T}}^{-1}(1-(\Delta T/\bar{\tilde{T}})]$ and $[\hat{\hat{\tilde{\dot{s}}}}/\hat{\hat{\tilde{d}}}(k)](1-(\Delta T/\bar{\tilde{T}})]$
define the slope of the family of dashed lines as a function of the abscissa and the ordinate passing though the origin in relation to the mean cold bias ΔT .

Air Temperature Differences

Mean Model